Molecular Therapy
Nucleic Acids
Original Article

Cas-CLOVER is a novel high-fidelity nuclease for safe and robust generation of T_{SCM}-enriched allogeneic CAR-T cells

Blair B. Madison,[1] Deepak Patil,[1] Maximilian Richter,[1] Xianghong Li,[1] Min Tong,[1] Stacey Cranert,[1] Xinxin Wang,[1] Renata Martin,[1] Haibin Xi,[1] Yening Tan,[1] Leslie Weiss,[1] Karl Marquez,[1] Julia Coronella,[1] Devon J. Shedlock,[1] and Eric M. Ostertag[1]

[1]Poseida Therapeutics Inc., 9390 Towne Centre Dr. #200, San Diego, CA 92121, USA

The use of T cells from healthy donors for allogeneic chimeric antigen receptor T (CAR-T) cell cancer therapy is attractive because healthy donor T cells can produce versatile off-the-shelf CAR-T treatments. To maximize safety and durability of allogeneic products, the endogenous T cell receptor and major histocompatibility complex class I molecules are often removed via knockout of T cell receptor beta constant (*TRBC*) (or T cell receptor alpha constant [*TRAC*]) and *B2M*, respectively. However, gene editing tools (e.g., CRISPR-Cas9) can display poor fidelity, which may result in dangerous off-target mutations. Additionally, many gene editing technologies require T cell activation, resulting in a low percentage of desirable stem cell memory T cells (T_{SCM}). We characterize an RNA-guided endonuclease, called Cas-CLOVER, consisting of the Clo051 nuclease domain fused with catalytically dead Cas9. In primary T cells from multiple donors, we find that Cas-CLOVER is a high-fidelity site-specific nuclease, with low off-target activity. Notably, Cas-CLOVER yields efficient multiplexed gene editing in resting T cells. In conjunction with the piggyBac transposon for delivery of a CAR transgene against the B cell maturation antigen (BCMA), we produce allogeneic CAR-T cells composed of high percentages of T_{SCM} cells and possessing potent *in vivo* anti-tumor cytotoxicity.

INTRODUCTION

Chimeric antigen receptor T (CAR-T) cell therapy is rapidly becoming an effective treatment for cancer, particularly for lymphocytic leukemias and multiple myeloma.[1,2] CAR-T therapies use T cells that are genetically modified to express a chimeric antigen receptor (CAR) that recognizes a specific antigen expressed on the surface of malignant cells. The use of primary T cells directly from patients avoids alloreactivity and exploits the excellent safety profile associated with an autologous transplant. However, there are a number of issues that may make autologous cells a suboptimal source for CAR-T manufacturing, including lower T_{SCM} percentages in aging patients and immune dysfunction due to the disease process or prior treatments.[3] Alternatively, allogeneic cells from younger, healthy donors could provide a universal source of pre-manufactured, off-the-shelf CAR-T cells if alloreactivity could be effectively mitigated.

Genetic manipulations of T cells are often pursued using a site-specific nuclease (SSN) for gene inactivation; e.g., when targeting T cell receptor alpha constant (*TRAC*) and *B2M* to inactivate the T cell receptor (TCR) and major histocompatibility complex class I (MHC-I) proteins for mitigating host-graft alloreactivity. This strategy usually relies on an SSN and subsequent error-prone double-strand break (DSB) repair. The fidelity of an SSN is critical for preserving cellular function and preventing oncogenic or other detrimental mutations derived from unintended off-target DSBs. The most commonly used RNA-guided Cas9 nuclease, from *Streptococcus pyogenes* (SpCas9), can yield significant levels of off-target activity,[4–9] with reported off-target cutting as high as 13%.[10] Multiplex editing with SpCas9 for CAR-T engineering can also lead to high rates of translocations, up to 4% for individual translocations or rearrangements and up to 5% cumulatively.[9–11]

For optimal therapeutic CAR-T function, a gene editing platform would ideally be compatible with the preservation of a high percentage of T_{SCM} cells. These cells possess self-renewing capacity, yield greater levels of engraftment, and drive more effective anti-tumor responses.[12–15] Adoptive immunotherapies are critically dependent on such function, with earlier studies suggesting that less differentiated T cells were much more effective.[15–17] Given the demonstrated advantages of T_{SCM} cells for CAR-T therapy, multiple efforts have focused on the development of specific protocols and methods to selectively enrich these desirable cells during CAR-T manufacturing.[18–23] To preserve the T_{SCM} subset during production of allogeneic CAR-T, a gene editing platform must perform efficiently in resting T cells, which has been a challenge for most gene editing platforms to date.[24,25]

Here we describe a dimeric, high-fidelity SSN, Cas-CLOVER, which consists of a fusion of catalytically dead SpCas9 (dCas9) with the nuclease domain from a *Clostridium* Clo051 type IIs restriction

Received 10 September 2021; accepted 8 June 2022;
https://doi.org/10.1016/j.omtn.2022.06.003.

Correspondence: Eric M. Ostertag, MD, PhD, Poseida Therapeutics, Inc., 9390 Towne Centre Dr., Suite 200, San Diego, CA 92121, USA.
E-mail: ostertag@poseida.com

endonuclease. This yields a nuclease whose activity is predicated upon the dimerization of the Clo051 nuclease domain, enabled by RNA-guided recognition of two adjacent 20-nt target sequences. Unlike a paired nickase approach, e.g., when using the Cas9-D10A mutant,[7] monomeric Cas-CLOVER does not introduce a nick or a DSB. We find that Cas-CLOVER has low off-target nuclease activity and is implemented here for targeted inactivation of the T cell receptor beta constant (*TRBC*) and *B2M* loci in primary human T cells to achieve TCR and MHC-I inactivation. In conjunction with the piggyBac transposon for transgenesis with a CAR specific for the B cell maturation antigen (BCMA), Cas-CLOVER enables the safe production of a fully allogeneic CAR-T product candidate, P-BCMA-ALLO1, with an exceptionally high T_{SCM} composition. P-BCMA-ALLO1 demonstrates robust anti-tumor activity *in vitro* and both anti-tumor activity and persistence in multiple animal models *in vivo*.

RESULTS

Generation and characterization of Cas-CLOVER

Cas-CLOVER was generated by fusion of the C-terminal nuclease domain of Clo051 to the amino terminus of catalytically inactive Cas9 (dCas9) via a flexible GGGGS (G4S) linker, with SV40 nuclear localization signals (NLSs) added at both the amino and carboxy terminus of this fusion protein (Figures 1A and 1B). Cas-CLOVER migrated by SDS-PAGE at a rate consistent with its predicted molecular weight of 185 kDa (Figure 1C). Nuclease activity was gauged with a reporter that yields GFP fluorescence after error-prone non-homology-mediated end joining (NHEJ) repair and formation of either insertions or deletions (indels) (Figure 1D). Various spacer lengths were compared between two *AAVS1* protospacer sequences and fluorescence was measured in Ad293 cells (Figures 1D–1F). A surveyor nuclease assay confirms the presence of indels at the endogenous *AAVS1* site, which contains a 17-nt spacer (Figure 1G).

Activity at an endogenous locus was assessed for the *TRAC* locus in Jurkat cells by measuring surface levels of CD3 via flow cytometry utilizing guide RNA (gRNA) pairs targeting protospacer sequences with various spacing. This allowed the assessment of Cas-CLOVER activity with various spacer lengths in the context of an endogenous gene (Figure 1H). In this experiment, a longer 20-amino-acid linker (G4S × 4) was evaluated, which revealed results similar to the shorter five-amino-acid G4S linker (Figure 1H).

Efficient gene disruption and knockins with Cas-CLOVER

For allogeneic CAR-T therapy, the mitigation of graft-versus-host disease (GVHD) and host-versus-graft disease (HGD) risk is often achieved by inactivation of the endogenous TCR and MHC-I molecules, respectively. We compared Cas9 and Cas-CLOVER for their ability to inactivate the *TRAC* region, beta-2-microglobulin (*B2M*) component of MHC-I, and the immune checkpoint receptor *PDCD1* (Figure 2A). The on-target efficiency of Cas-CLOVER was on par with Cas9 at each site, and not significantly different. As desired for a fully dimeric system, Cas-CLOVER exhibited no activity when either gRNA was supplied alone (Figures 2A and 2B), generating no DSBs by either half of the dimeric system.

For production of fully allogeneic P-BCMA-ALLO1 CAR-T cells, we use piggyBac to deliver the CAR transgene and the Cas-CLOVER nuclease to perform multiplexed knockouts of *B2M* and the *TRBC* region genes (Figure 2C). The transposase enzyme is provided as mRNA along with the transposon vector (Figure 2D). Cas-CLOVER is supplied as mRNA with additional gRNAs specific for *B2M* and *TRBC*. All reagents are added via an electroporation step to resting T cells. The quiescent status of T cells was validated by examining proliferation by dye dilution, as assessed by flow cytometry (Figures S1A–S1D). CAR expression was evaluated at day 5, revealing a transposition efficiency of 25%–30% (Figure S1E), while methotrexate (MTX) selection yielded a population with about 90% of cells CAR positive (Figure S1F). Comparison of CAR expression (Figures S1E and S1F) and cellular expansion (Figure S1F) revealed no significant differences between gene-edited and unedited CAR-T cells. TCR and B2M protein loss were evaluated following the purification step in Figure 2C. Note that, during the purification step, any remaining TCR-positive cells are removed via negative selection, to help mitigate the risk of GVHD. Removal of MHC-I-positive cells is not performed, thereby creating a product that is nearly entirely composed of TCR-negative cells but contains a mixture of MHC-I-positive and MHC-I-negative cells. TCR inactivation across multiple donors was assessed by CD3 expression, and, after purification, TCR knockout levels were 99% and higher (Figure 2E). On-target indels were evaluated by amplicon sequencing (amplicon-seq) at the *TRBC* and *B2M* Cas-CLOVER cut sites (Figures S2A–S2F). Among purified CAR-T cells, indel levels across donor lots varied between 94% and 99% at *B2M*, and *TRBC1*/*TRBC2* loci (Figure 2F). These data demonstrate that Cas-CLOVER yields efficient multiplexed knockouts in resting human T cells.

To determine HDR (homology-directed repair)-mediated knockin potential using Cas-CLOVER, we examined reporter cassette delivery at several loci (*GAPDH*, *B2M*, and *HBB*) in proliferating induced pluripotent stem cells (iPSCs). Cas-CLOVER mRNA, gRNA, and donor DNA were delivered by electroporation. For targeting *GAPDH*, an in-frame GFP cassette was integrated into exon 2 (Figure S3A). SSN cutting was validated (Figure S3B) and fluorescence evaluated. Targeting efficiency was similar between Cas-CLOVER and HiFi-Cas9 (Figures S3C and S3D), as also observed at the *B2M* locus (Figure S3E). At *HBB*, knockin efficiency was higher using Cas-CLOVER, which was not likely due to differential efficiency of target cleavage as gauged by indel generation (Figure S3F). Cas-CLOVER thus appears to yield cassette cargo integration at least as efficiently as HiFi-Cas9.

Very low off-target activity of the Cas-CLOVER nuclease

Given the justifiable concern for off-target nuclease activity, we implemented a multiple inverted index *in silico* prediction algorithm[26] to nominate candidate off-target sites for *TRAC*, *B2M*, and *PDCD1*. Off-target sites were selected based on possible dual and single gRNA occupancy scenarios (Figure S4A). Following electroporation of resting pan-T cells, candidate off-target sites were queried for the presence of indel mutations by PCR amplification and Illumina-based

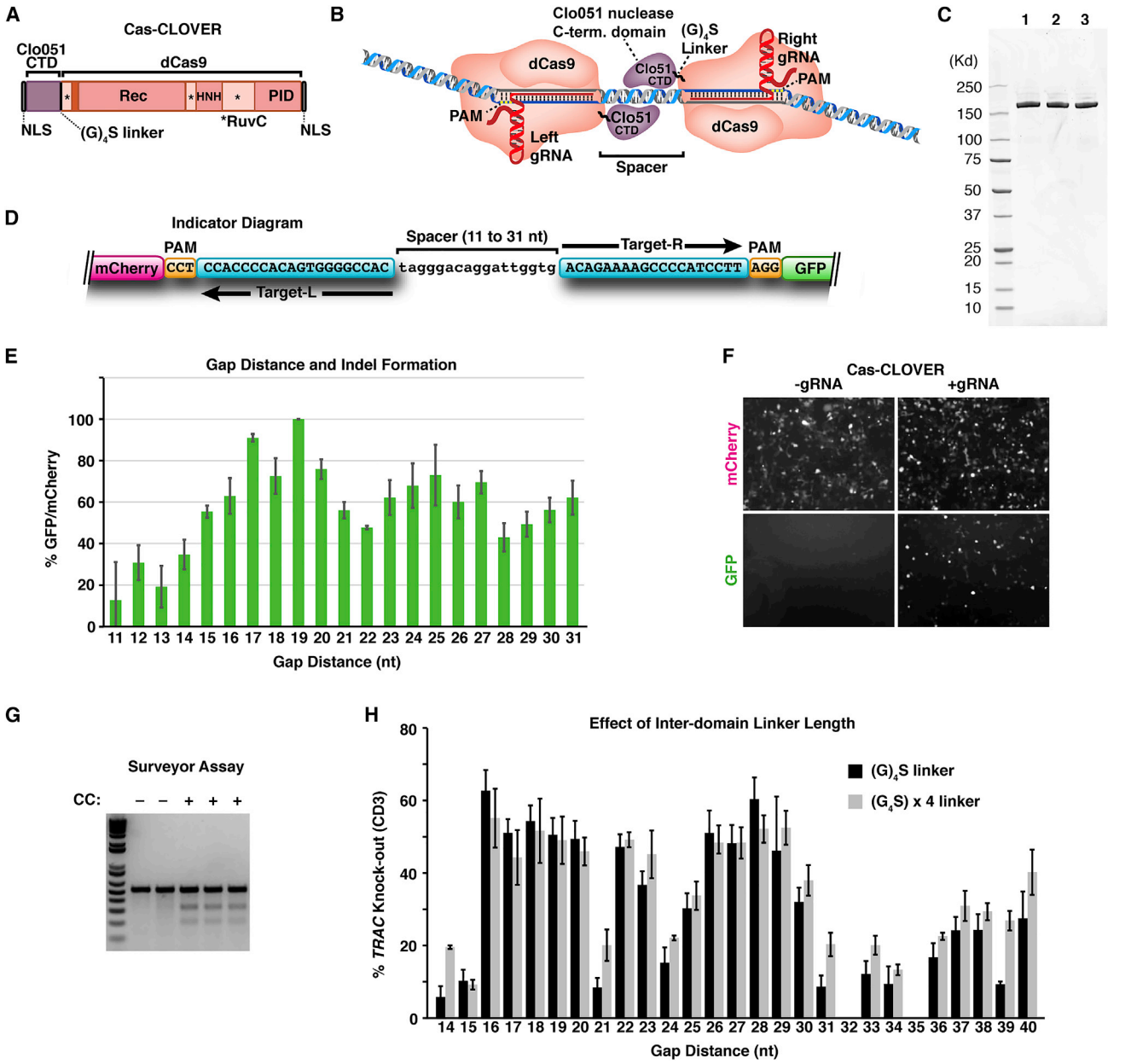

Figure 1. Cas-CLOVER is an efficient dimeric nuclease

(A) Cas-CLOVER consists of a fusion of the carboxy terminal nuclease domain of Clo051 linked to the amino terminus of dCas9 via flexible GGGGS (G4S) linker. (B) Schematic of the dimeric Cas-CLOVER complex with DNA. Cleavage of DNA depends on gRNA-directed binding of two protospacers in target sequence, followed by Clo051-mediated cleavage within the spacer between each monomer. (C) Three replicates of purified Cas-CLOVER protein (1 μg) were run on SDS-PAGE and stained with SYPRO Orange. Cas-CLOVER migrated at a rate consistent with its predicted molecular weight of 185 kDa. (D) NHEJ indicator reporter with *AAVS1* target protospacer sequence containing varying lengths of a spacer sequencing containing one or two stop codons, located between an mCherry and EGFP ORF. (E) Percentage GFP-positive cells as a proportion of mCherry-positive Ad293 cells 24 h after co-transfection of Cas-CLOVER and *AAVS1*-specific gRNAs. (F) Immunofluorescence images of mCherry and EGFP fluorescent cells. (G) Surveyor mutation detection assay reveals cleavage in *AAVS1* target sequences following transfection of HEK293 cells with Cas-CLOVER (CC) and gRNAs. (H) Assessment of TCR knockout in Jurkat leukemia T cell line as determined by staining against CD3 and flow cytometry, with varying spacing between each protospacer target pair in the *TRAC* locus, using Cas-CLOVER with a G4S or 20 amino acid G4S × 4 linker. Error bars in E and H represent standard error of the mean among technical replicates.

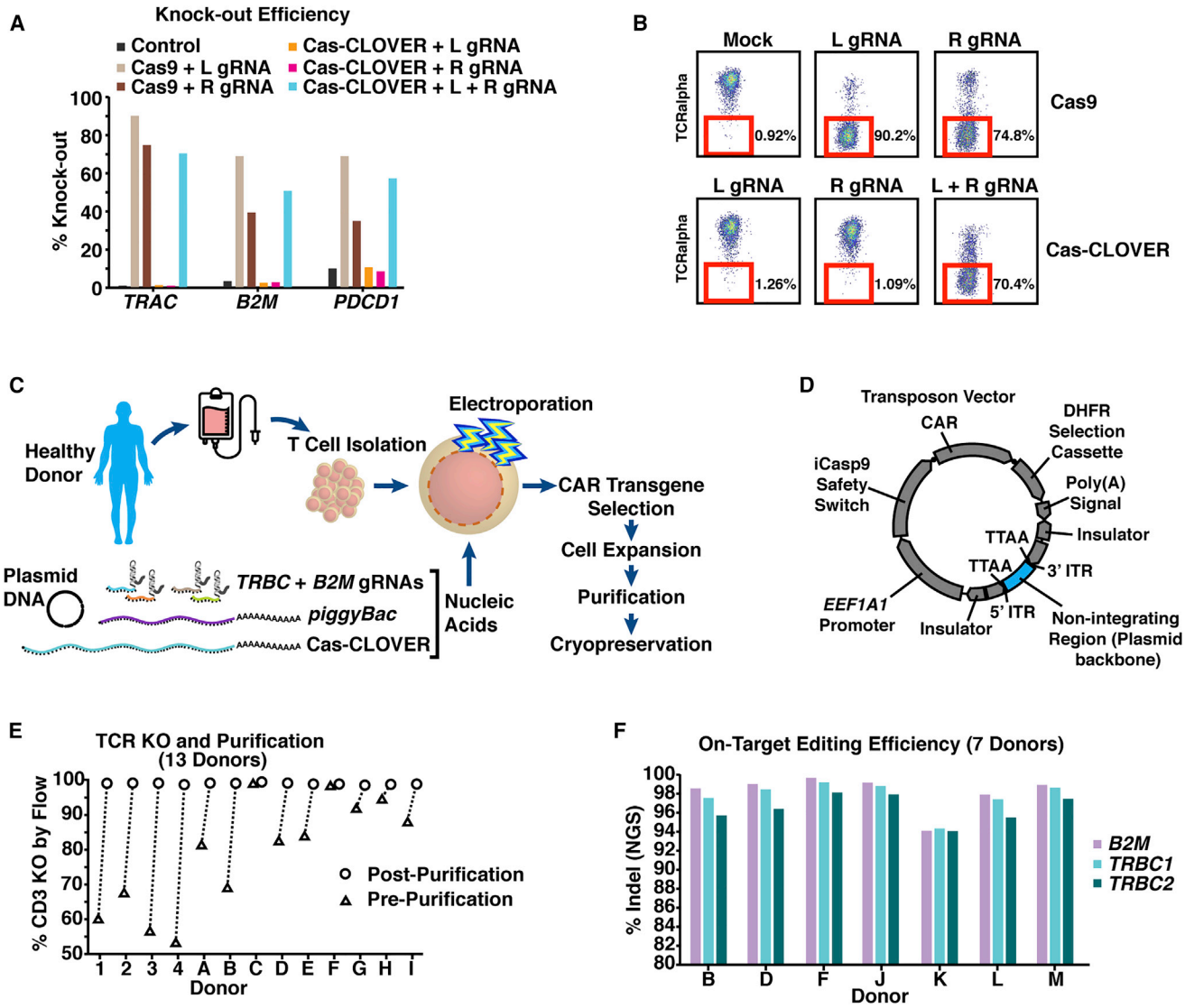

Figure 2. Cas-CLOVER yields efficient knockouts in primary human T cells

(A) Comparison of Cas9 with Cas-CLOVER nucleases for inactivation of *TRAC*, *B2M*, and *PDCD1* loci, with one or two gRNAs. (B) Flow cytometry scatterplots of knockout of *TRAC* reveals the strict requirement of two targeting gRNAs for Cas-CLOVER activity, unlike Cas9. (C) Manufacturing process for production of CAR-T cells with targeted inactivation of the *TRBC* and *B2M* loci. (D) Plasmid map of the CAR transgene in a transposon vector, also containing expression cassettes for a DHFR (dihydrofolate reductase) selection marker and inducible Caspase-9 (iCasp9) safety switch, all driven by the *EEF1A1* promoter. (E) Percentage TCR inactivation in CAR-T cells as determined by expression of CD3 across multiple human donor lots, before and after purification of TCR-negative cells. (F) Measurement of indels in targeted loci by NGS following purification of TCR-negative CAR-T cells.

next-generation sequencing (NGS) (amplicon-seq). For all loci queried, including *TRAC* and *B2M* (Figures S4B and S4C), and *PDCD1* (not shown), indel frequency at candidate off-target sites did not occur at a statistically significant level above background. Therefore, off-target activity at these sites is extremely low and highlights the high fidelity of the Cas-CLOVER nuclease.

To supplement *in silico* prediction methods, we pursued unbiased double-stranded oligodeoxynucleotide (dsODN) capture in human T cells. This genome-wide, unbiased identification of double-strand DNA breaks enabled by sequencing (GUIDE-seq) entails the capture of dsODNs after nuclease cleavage.[27] We used a modified version of this protocol called iGUIDE.[28] The procedure we pursued for GUIDE-seq was essentially identical to our process for producing *TRBC* and *B2M* double-knockout CAR-T cells from primary human T cells, except for the additional electroporation of the dsODN (Figure 3A). Five donor lots of resting primary human T cells were used for the GUIDE-seq workflow to generate a

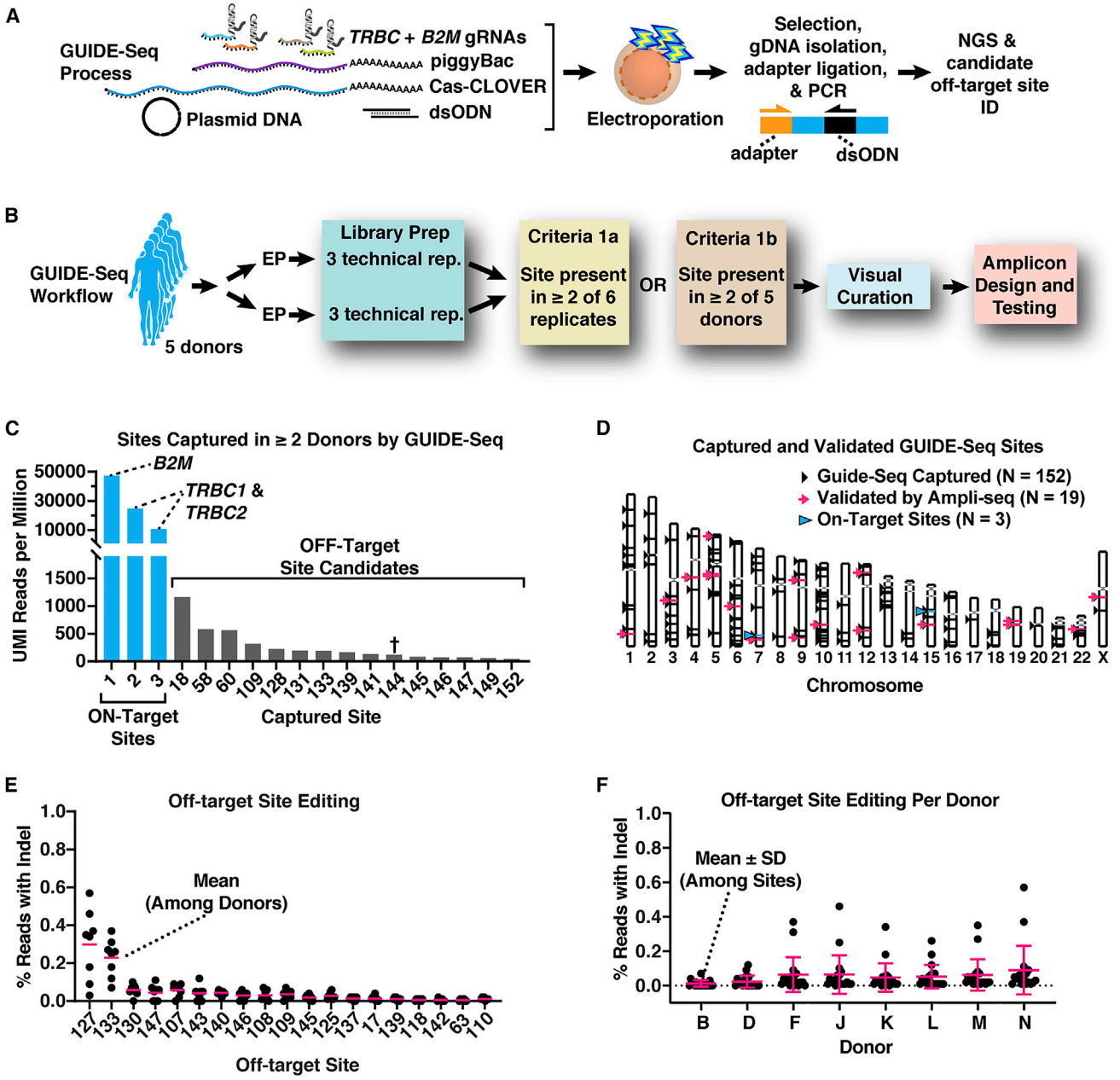

Figure 3. Identification and assessment of Cas-CLOVER off-target sites

(A) GUIDE-seq procedure in T cells entails electroporation of gRNAs and a dsODN along with other components for allogeneic CAR-T production, followed by detection of captured sites by NGS. (B) Experimental workflow for GUIDE-seq analysis and validation. (C) Genomic locations captured via GUIDE-seq as quantified by UMI reads obtained for sites present in at least two donor T cell lots. One site (†) could not be validated by amplicon-seq because of inability to PCR amplify this genomic region. (D) Chromosomal maps of human genome with demarcation of all GUIDE-seq captured sites, validated sites, and on-target sites. (E) AmpliSeq results of 19 sites exhibiting detectable levels of indels, as measured by NGS. (F) Levels of off-target activity across eight donors as measured by AmpliSeq for 19 validated GUIDE-seq sites, with mean indel frequencies plotted.

candidate list (Figures 3B and 3C). Candidate off-target sites were found on all 22 autosomes and the X chromosome (Figure 3D), which were subsequently interrogated by amplicon-seq (Figures S5A and S5B). Indel rates were only detectable among 19 sites across CAR-T lots produced from eight separate donors, with only two sites (GS127 and GS133) yielding indel rates above background levels of 0.1% (Figures 3E and S5C). Average off-target indel mutation rates varied from donor to donor, with average

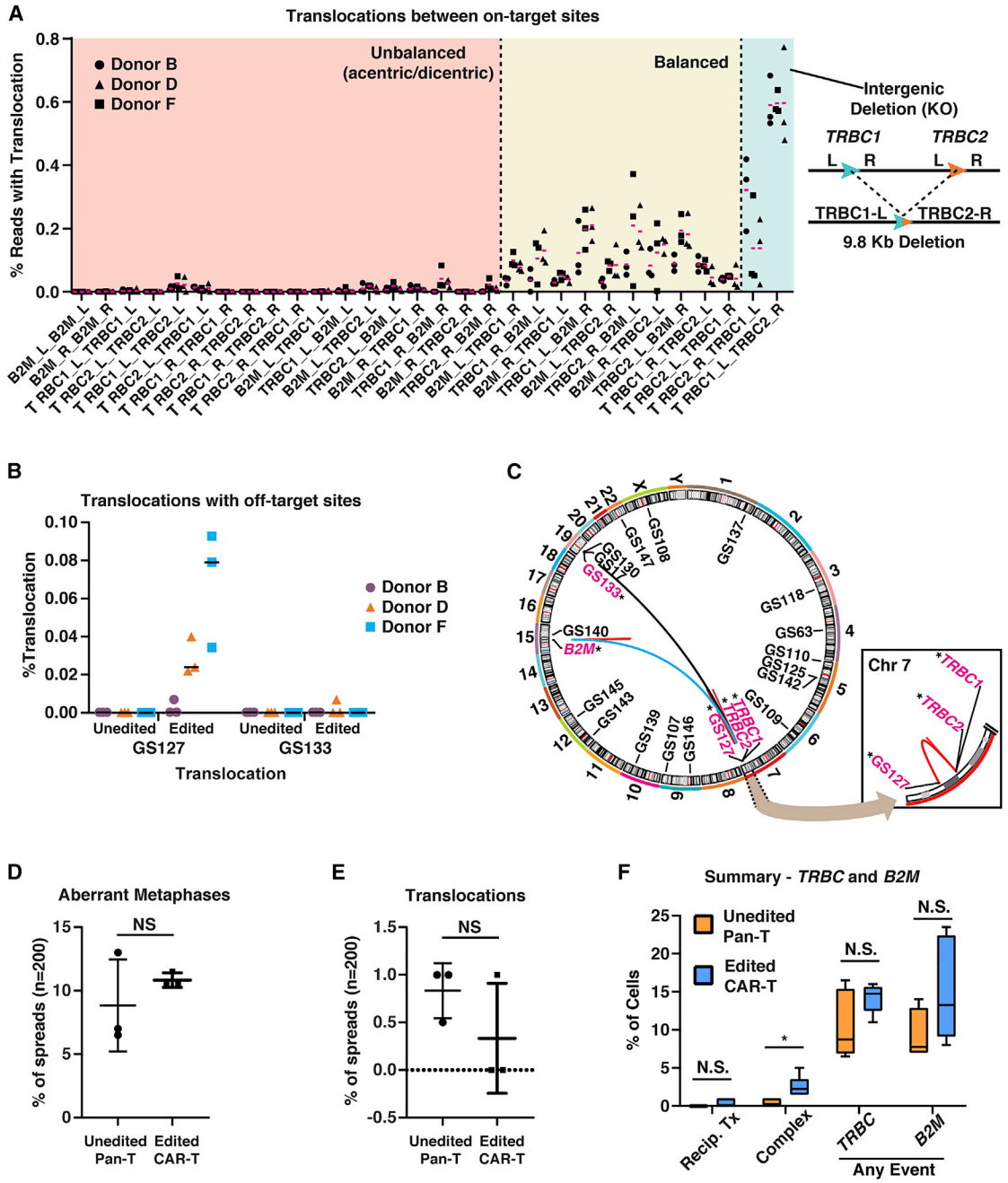

Figure 4. Quantifying translocations and genome stability

(A) Results from AMP-seq showing levels of unbalanced and balanced translocations between *TRBC1*, *TRBC2*, and *B2M*, including intergenic deletion between *TRBC1* and *TRBC2* for three donors. (B) Results from AMP-seq revealing low levels of translocations between on-target sites and GS127 and GS133. (C) Circos plot of donor D cells showing translocations between *B2M*, *TRBC1*, *TRBC2*, GS127, and GS133 off-target sites. Results from karyotype analysis from three lots of unedited pan-T and edited allogeneic CAR-T show no differences in aberrant metaphase spreads (D) and no difference in total translocations (E) by a two-tailed paired t test. (F) Summary of results from high-resolution dGH-FISH at *TRBC* and *B2M* edit sites. A two-tailed paired t test was implemented to determine significance between unedited pan-T and edited CAR-T cells; *p < 0. 05. Error bars in D, E, and F represent standard deviation from the mean.

indel rates among donors ranging between 0.012% and 0.089% (Figure 3F), all in the context of on-target indel rates of 92%–99% (Figure 2G). This low rate of indel formation at off-target sites in T cells appears lower than off-target indel rates reported using CRISPR-Cas9 to generate knockouts in primary human T cells.[8,9]

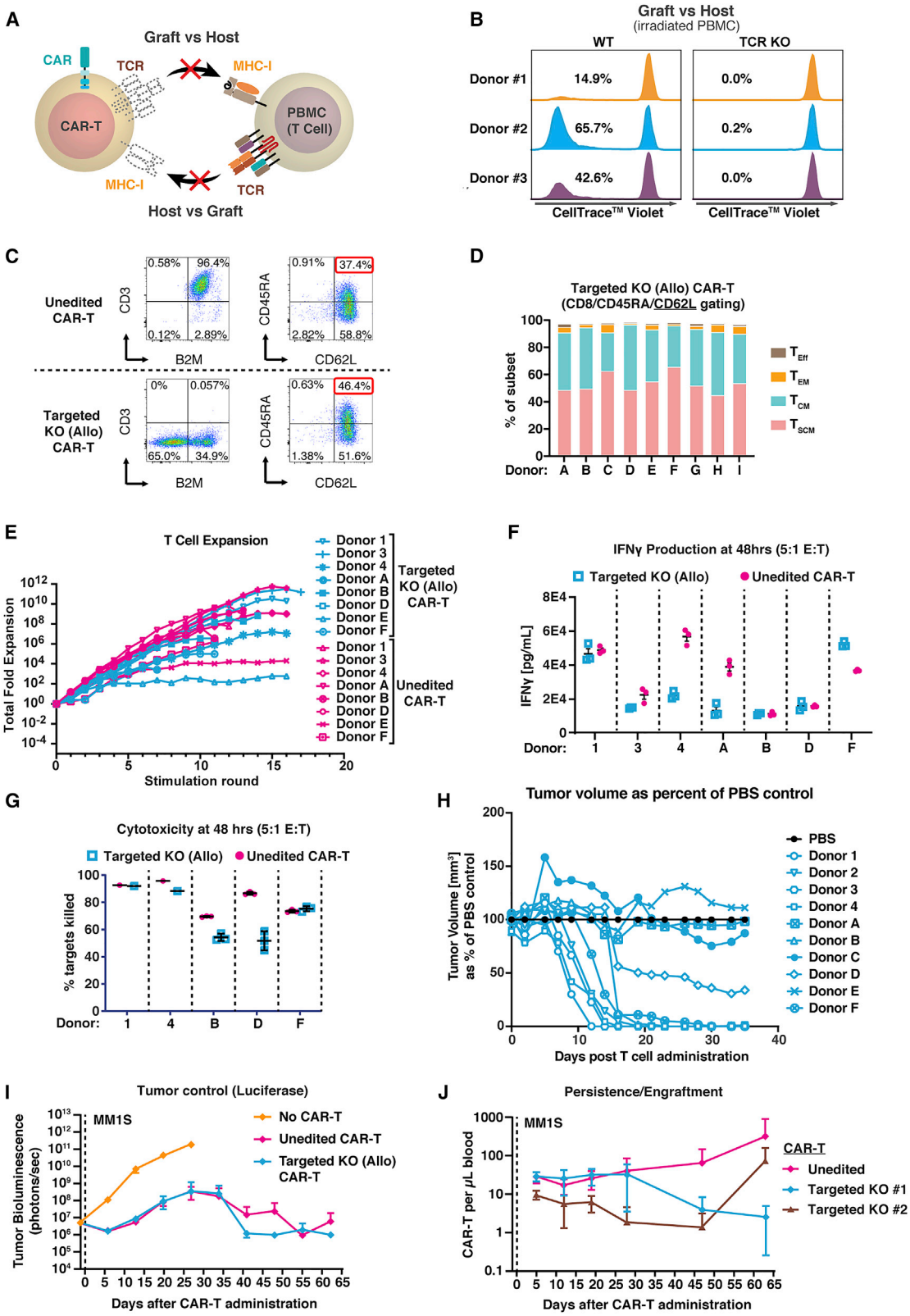

(legend on next page)

Cas-CLOVER editing maintains genome stability and a normal karyotype in T cells

We examined translocation species using anchored multiplex PCR and NGS (AMP-seq),[29] whereby translocations between on-target edit sites are captured and quantified, in addition to those that may occur between on-target and off-target edit sites. On-target translocation rates are depicted in Figure 4A, with unbalanced translocations being the rarest and often undetectable. Balanced translocations could also be observed, with most donors and sites at a rate of 0.2% or lower (Figure 4A). Intergenic deletions were also observed between *TRBC1* and *TRBC2* edit sites, likely generating a null allele (Figure 4A). Translocations of on-target sites with off-target sites curated by GUIDE-seq and amplicon-seq (Figures 3C, 3E, and 3F) were detected only with GS127 and GS133 by AMP-seq (Figures 4B and 4C). These rates of translocations are 5- to 10-fold lower than that reported previously using Cas9 and TALEN nucleases.[9–11,30,31]

Metaphase G-banding karyotype analysis of edited CAR-T cells also revealed no significant difference between CAR-T cells and unedited pan-T cells, regarding any aberration (Figure 4D), including translocations (Figure 4E). To more closely examine chromosomal integrity, we pursued directional genomic fluorescent *in situ* hybridization (dGH-FISH).[32,33] In this approach, sequences flanking each edit site at *TRBC* and *B2M* were probed, along with whole-chromosome painting of chromosomes 1, 2, and 3 (Figures S6A and S6B). There was an insignificant trend for increased translocation between each edit site (Figures 4F, S6D, and S6E) and a small but significant increase in complex rearrangements for *TRBC* (Figures 4F and S6D), but no significant increase in any other abnormality (inversion, sister-chromatid exchange, deletion, gain, or insertion) (Figures S6C–S6E). Overall, these assays indicate that CAR-T cells generated using Cas-CLOVER largely retain genome integrity.

Cas-CLOVER editing does not compromise the CAR-T phenotype

Inactivation of the TCR is expected to render T cells unresponsive to mismatched peripheral blood lymphocytes (PBMCs) (Figure 5A); this is evident when CAR-T cells are produced as in Figure 2C, which are double knockouts (DKO) of both *TRBC* and *B2M* (but purified to remove any TCR-positive cells). Such CAR-T cells do not proliferate upon exposure to mismatched irradiated PBMCs (Figure 5B). We have demonstrated that purification to remove any MHC-I-positive cells will likewise mitigate host-versus-graft alloreactivity in the reverse mixed lymphocyte reaction (data not shown). However, we do not purify P-BCMA-ALLO1 by MHC-I negative selection and thereby maintain MHC-I function in approximately one-third of the CAR-T cells in the final product (Figure 5C). This is done to determine whether this fraction will survive longer *in vivo* due to a possible host natural killer (NK) cell response to the MHC-I-negative cells.

CAR-T cells produced via piggyBac transposon transgenesis, starting with resting pan-T cells, have a high percentage of stem cell memory T cells (T_{SCM}), with some donors yielding over 60% T_{SCM} (Figures 5C and 5D). CAR-T cells with Cas-CLOVER-mediated inactivation of *TRBC* and *B2M* also maintain a very large proportion of the T_{SCM} subset (Figures 5C, 5D, S7A, and 7B). *In vitro* assays showed that these KO cells produced as an allogeneic CAR-T therapy against the BCMA antigen exhibited robust proliferation upon serial restimulation (Figure 5E), secreted high levels of interferon-gamma (IFNγ) (Figure 5F), and killed BCMA-expressing tumor cells (Figure 5G). Most critically, we see robust *in vivo* activity of allogeneic CAR-T cells produced from multiple donors using Cas-CLOVER, in which BCMA-expressing tumors were eliminated in xenografts in immunocompromised mice for seven out of 10 donors (Figure 5H). Remarkably, in a challenging MM.1S tumor model, BCMA-ALLO CAR-T cells show enduring tumor control (Figures 5I and 5J), which underscores their persistence and robust anti-tumor activity, *in vivo*. These data show that allogeneic CAR-T cells produced with piggyBac and Cas-CLOVER have an excellent safety profile, with potent anti-tumor cytotoxicity likely stemming from the high proportion of T_{SCM} cells.

DISCUSSION

Allogeneic CAR-T therapies have the potential to dramatically increase patient access and decrease production costs for the treatment of a variety of malignancies. The pre-selection of optimal donor profiles is also a key advantage for allogeneic approaches. However, an effective allogeneic approach is critically dependent on clean and efficient gene editing; product safety hinges on the fidelity of the intended genetic manipulations in T cells. Cas-CLOVER yields high fidelity in comparison with other SSNs used in the production of allogeneic CAR-T cells. Considering the rapidly changing landscape of

Figure 5. Favorable phenotype of edited allogeneic CAR-T cells

(A) Schematic of CAR-T cells manipulated for inactivation of the TCR and MHC-I proteins for functional mitigation of alloreactivity. (B) Proliferation assay results measuring alloreactivity (graft versus host) of unedited (WT) versus TCR knockout (KO) CAR-T cells as measured by CellTrace Violet dilution in a mixed lymphocyte reaction. (C) Flow cytometry of unedited (WT) CAR-T and *B2M*/*TRBC* double-KO CAR-T cells stained for CD3, B2M, CD45RA, and CD62L. (D) Proportion of different T cell phenotypic subsets (T_{SCM}, T_{CM} (central memory), T_{EM} (effector memory), and T_{EFF} (effector)) among targeted KO (Allo) CAR-T cells. Targeted KO CAR-T cells were further profiled for cellular expansion (E), interferon gamma (IFNγ) secretion (F), *in vitro* BCMA-K562 tumor cell killing (G), and *in vivo* RPMI-8226 tumor elimination in a mouse xenograft model (H), which revealed no compromised function in targeted KO CAR-T cells (N = 6 per group). (I) Allogeneic anti-BCMA CAR-T cells produced using Cas-CLOVER showed anti-tumor efficacy comparable with non-gene-edited CAR-T cells in the systemic MM.1S xenograft model of multiple myeloma. (J) Cas-CLOVER edited allogeneic (targeted KO) anti-BCMA CAR-T cells were detectable in the peripheral blood of treated animals throughout the duration of the study, as were unedited CAR-T cells, thus demonstrating durability of both edited and unedited CAR-T cells. Shown are mean ± 95% confidence interval (CI). All *in vitro* assays were performed in triplicate except for donor 1 and 4 in (G). *In vivo* tumor studies were performed with n = 6 mice per group. *In vitro* assays were not performed on donor #2 (E, F, and G), donor #3 (G), donor A (G), donor C, (E, F, and G), or donor E (F and G) because of insufficient material. T cell expansion, IFNγ secretion, and cytotoxicity were not significantly different between edited and unedited CAR-T cells, by a paired two-tailed t test. Error bars in I and J represent standard deviation from the mean within animal groups.

engineered SSNs, thorough scrutiny is necessary to identify off-target effects. To account for genetic variability, multiple donors and production lots should be examined, especially in the context of a larger panel of potential off-target sites. To our knowledge, neither variability across different genetic backgrounds nor effects on T_{SCM} composition have been examined in allogeneic CAR-T gene editing studies.

Currently available data do provide some insight into the fidelity of SSNs used for targeted mutagenesis in T cells,[8,9,34] but few studies have queried off-target activity after candidate site nomination by unbiased methods. *In silico* prediction methods can fail to identify off-target nuclease cutting or base editing activity,[10,27] while GUIDE-seq alone does not provide a readout of frank off-target mutagenesis. Some allogeneic CAR-T studies have performed GUIDE-seq to identify potential off-target sites,[10,35] but such sites should be validated and off-target mutations directly quantified. At off-target sites, Cas-CLOVER does not yield off-target nuclease activity above 0.6% among eight donors and 140 queried sites. For the majority of donors (75%), off-target activity did not exceed 0.4% (Figures 3E and 3F). Thus, high-fidelity gene editing is achieved with Cas-CLOVER, with a level of fidelity possibly up to 25-fold greater than CRISPR-Cas9.[8,10]

Further head-to-head comparisons may be needed, but Cas-CLOVER appears to be among the highest-fidelity nucleases used for gene editing. Other SSNs engineered for high fidelity, such as enAs-Cas12a-HF1 and HiFi-Cas9,[36,37] reportedly yield high fidelity in gene-edited T cells, with maximal off-target rates below 0.1% for HiFi-Cas9.[37] However, in this study, off-target sites for HiFi-Cas9 were nominated with *in silico* prediction algorithms and not by unbiased methods such as GUIDE-seq.[37] Current base editors yield fidelity approaching that of Cas-CLOVER, with cytosine base editing in T cells yielding a maximal off-target editing rate of 0.9% using a fourth-generation base editor (BE4).[10] However, this is likely to be context (or donor) dependent, since recent reports document much higher levels of off-target mutations (1.55%–7.63%) in T cells engineered using a third-generation base editor (BE3).[38] Other reports have highlighted the need to eliminate off-target effects of APOBEC-derived base editors,[39–42] which can yield high levels of off-target editing in both RNA and DNA.[39,42–46] In the future, the application of such high-fidelity base editors in CAR-T cells may yield specificity similar to that observed for Cas-CLOVER.

While Cas-CLOVER is the central focus of this study, the piggyBac transposon also has a favorable safety profile. PiggyBac has a lower tendency to disrupt genes, compared with lentiviral vectors,[47,48] with most integrations avoiding expressed genes, and having a greater preference for safe harbor sites.[49] The large cargo capacity of piggyBac also enables the addition of a safety switch, such as an inducible Caspase-9,[50,51] which enables specific elimination of CAR-T cells, if needed. Further contributing to safety, the prevention of GVHD of final BCMA-ALLO CAR-T cells is optimized through pre-selection of donors, which typically yield 60% or higher T_{SCM} composition, >99% TCR-negativity, and ~67% B2M/MHCI-negativity.

One clinical trial for B cell malignancies using piggyBac to generate CAR-T cells documented T cell transformation. However, this event was likely not driven by classical insertional mutagenesis, as concluded by the authors themselves.[52,53] Rather, contributing factors likely included process-related parameters, such as DNA-damaging high-voltage electroporation conditions, and patient-specific exacerbating conditions, such as GVHD caused by the allogeneic source of donor PBMCs. High vector copy numbers (20–30 copies) were also observed in this study,[52,53] in contrast to what we observe in our process, which maintains low vector copy numbers (about two or three copies, on average).

In addition to the high fidelity of the Cas-CLOVER nuclease and favorable safety profile of the piggyBac transposon, an additional advantage is the ability to perform robust multiplexed gene editing in resting T cells. Gene editing in non-dividing T cells likely helps maintain genome integrity. Double-strand DNA breaks created by SSNs in dividing cells are frequently not repaired prior to chromosomal segregation.[54] This can lead to loss of a chromosomal arm, micronuclei formation, dicentric bridges, or chromosome breakage.[54] In terms of function, gene editing in resting T cells helps preserve a T_{SCM}-enriched product and maintain high replicative potential, thereby producing a fully allogeneic product with robust anti-tumor activity. When using optimal donors, P-BCMA-ALLO1 is typically >99% TCR negative, >95% CAR positive, and consists of 50%–70% T_{SCM} cells. We believe that high-T_{SCM} fully allogeneic CAR-T products will be essential to maximize efficacy, durability, and safety in the clinic.

MATERIALS AND METHODS

Generation of Cas-CLOVER

Clo051 is a predicted type IIs restriction enzyme from *Clostridium* (CDB: 15833). The Cas-CLOVER protein expression plasmid was generated from a pUC19 vector using the CMV-Actin *Gallus gallus* (CAGG) promoter. The C-terminal nuclease domain (CTD) of Clo051 (E389-Y587, 199 amino acids) was inserted upstream of the catalytically dead mutant Cas9 endonuclease (dCas9) and linked with a five-amino-acid linker of G4S (GGAGGCGGGGGAAGC). The Clo051-dCas9 (Cas-CLOVER) fusion protein also has two SV40 large T antigen NLSs, one each at the N terminus and C terminus.

Assaying spacer length requirements of Cas-CLOVER

The *AAVS1* wild-type (WT) indicator vector, with mCherry and GFP co-expression open reading frames (ORFs), is driven by the cytomegalovirus (CMV) promoter with a linker containing an *AAVS1* target site. The target site was generated via Gibson assembly (New England BioLabs, Ipswich, MA) using NheI and XbaI restriction endonuclease-digested plasmid backbone and a gBlock fragment (Integrated DNA Technologies, Coralville, IA) containing the target sequences. The linker between the mCherry and EGFP ORFs consists of 59 base pairs from the *AAVS1* locus (*PPP1R12C*, chr19:55115725-55115783, hg38) flanked by EcoRI and BamHI restriction sites. A series of fluorescent indicator plasmids with varying synthetic spacer

lengths (all including one or two stop codons) were generated by cloning annealed duplex oligos (Integrated DNA Technologies) into the EcoRI and BamHI sites. Expression of the *AAVS1*-specific gRNAs in Ad293 cells was achieved by cloning the U6 promoter, *AAVS1*-specific spacers, and the invariant scaffold gRNA sequence into the pUC19 vector. The gRNA spacer (target) sequences corresponding to the *AAVS1* sequences in the human genome (hg38 reference) are chr19:55,115,764-55,115,783 (left gRNA site) and chr19:55,115,728-55,115,747 (right gRNA site).

For assays of various synthetic spacer lengths using the fluorescent reporter Ad293, cells were seeded into 24-well plates at a density of 1×10^5 cells per well in 500 μL of culture medium. The next day, 180 ng of mCherry-linker-GFP indicator plasmid DNA was co-transfected with 110 ng of *AAVS1* L gRNA, 110 ng of *AAVS1*-R gRNA plasmid, and 400 ng of Cas-CLOVER plasmid using Lipofectamine 2000 (Thermo Fisher, Waltham, MA). Three days (72 h) after transfection, cells were detached, washed, suspended in fluorescence-activated cell sorting (FACS) buffer (phosphate buffered saline [PBS] + 2% fetal bovine serum [FBS] + 0.1mM EDTA) for flow cytometry. Experiments were repeated for a total of three culture replicates.

For assays of various endogenous spacer lengths through *TRAC* knockout in Jurkat cells (ATCC), cells were washed with Opti-MEM reduced-serum medium (Thermo Fisher). For each electroporation transfection, 5×10^6 cells were electroporated with 20 μg of Cas-CLOVER mRNA in 100 μL of Opti-MEM using the BTX electroporation system (BTX, Holliston, MA) at 300 V for 700 μs. Transfected cells were transferred to six-well culture plates and maintained in culture for 2 days. Two days later, Cas-CLOVER-electroporated cells were pooled and washed again for electroporation with *TRAC*-specific gRNAs. Templates for gRNA *in vitro* transcription (IVT) were produced by PCR. Cells were electroporated with 10 μg of gRNA (5 μg left gRNA and 5 μg right gRNA) as performed for the Cas-CLOVER mRNA. Electroporated cells were transferred to 12-well plates and cultured for 3 days. Cells were then washed with PBS and stained with an anti-hCD3-APC antibody (BioLegend, San Diego, CA) in FACS buffer (PBS + 2% FBS + 0.1mM EDTA) followed by flow cytometry. Experiments were repeated for a total of three biological replicates. The genomic locations (hg38) for the 25 sites targeted at the *TRAC* locus on Chr 14 are 22550606 (60 nt), 22550564 (60 nt), 22550609 (62 nt), 22550603 (63 nt), 22550609 (64 nt), 22550606 (64 nt), 22550606 (66 nt), 22550606 (67 nt), 22550603 (67 nt), 22550597 (69 nt), 22550603 (70 nt), 22550620 (71 nt), 22550620 (72 nt), 22550620 (73 nt), 22550597 (74 nt), 22550597 (75 nt), 22550579 (75 nt), 22550609 (77 nt), 22550606 (79 nt), 22550606 (80 nt), 22550603 (82 nt), 22550541 (83 nt), 22550541 (84 nt), 22550606 (85 nt), and 22550606 (86 nt). The nucleotide span of each site, including protospacer adjacent motif (PAM) and space between protospacer, is indicated in parentheses.

Surveyor mutation detection assay

Ad293 cells in 24-well plates were transfected with 500 ng of the CAGG-driven Cas-CLOVER plasmid, 150 ng of *AAVS1* left gRNA plasmid, and 150 ng of *AAVS1* right gRNA plasmid with Lipofectamine 2000 at a 2.5:1 reagent-to-DNA ratio (Thermo Fisher). As a negative control pcDNA3.1 plasmid DNA was transfected. Genomic DNA was extracted from cells 72 h after transfection using the QuickExtract DNA Extraction Solution (Lucigen, Middleton, WI). The *AAVS1*-specific locus was amplified by PCR using primers specific for the targeted *AAVS1* site (forward, GGTCCGAGAGCTC AGCTAGT, and reverse, GATCAGTGAAACGCACCAGA) using the GoTaq PCR Master Mix (Promega, Madison, WI). The 514-bp PCR amplicon was denatured, hybridized, and digested using the Surveyor Mutation Detection Kit (Integrated DNA Technologies) following the manufacturer's instructions. DNA fragments were then separated by electrophoresis on a 2% agarose gel for analysis.

Production of mRNAs for Jurkat and T cell electroporation

For experiments in Jurkats and T cells, Cas-CLOVER was supplied as an *in vitro* transcribed RNA via electroporation. Using standard molecular biology techniques, the ORFs for Cas-CLOVER and super piggyBac (SPB) transposase were cloned into a T7-based IVT vector (pRT) upstream of an 80-nucleotide poly(A) tail and a SpeI site. For production of mRNA, 10 μg of plasmid DNA were linearized overnight with 200 U of SpeI-HF (New England Biolabs). DNA was then purified with the Qiagen QIAquick PCR purification kit (Qiagen Labs, Hilden, Germany). RNA was produced with the mMessage mMachine T7 Ultra Kit (Thermo Fisher) using 166.6 ng of linearized DNA per 20-μL reaction according to the manufacturer instructions for 3 h at 37°C. Polyadenylation of mRNA was achieved using the mMessage mMachine T7 Ultra Kit by incubating DNase-treated IVT reactions with *Escherichia coli* polynucleotide adenylyltransferase at 37°C for 1 h. The RNA generated was purified using the RNeasy Mini Kit (Qiagen) and yield and concentration were determined using a Nanodrop spectrophotometer (Thermo Fisher).

For Jurkat electroporations, gRNAs were produced by IVT following synthesis of an IVT template by PCR. Forward primers for this PCR amplification contained sequences for the T7 promoter, the TRAC-specific spacer, and for gRNA scaffold-specific priming, and are listed in Table S1. The reverse primer (AAAAGCACCGACTCGGTGCC) was designed for universal priming of the 3′ region of the gRNA scaffold sequence, which was cloned into pUC19 and used as template DNA for PCR. PCR fragments were generated with the Q5 High-Fidelity 2X Master Mix (New England Biolabs). Purified PCR amplicons were used for mRNA synthesis using the HiScribe T7 Quick High Yield RNA Synthesis Kit (New England Biolabs) following manufacturer's instructions.

To compare the effect of the linker length in Jurkat cells, a 20-amino-acid linker was cloned into the Cas-CLOVER plasmid (already containing the shorter five-amino-acid G4S linker) via Gibson assembly (New England Biolabs). A gBlock fragment from IDT (Integrated DNA Technologies) encoding the longer 20-amino-acid G4S (×4) linker (ggaggcgggggaagcGGCGGCGGAGGGAGCGGCGGAGGAG GCAGCGGCGGAGGCGGCAGC) was cloned at the MunI and

SbfI restriction endonuclease sites in the Cas-CLOVER plasmid by standard techniques. These T7 promoter-driven Cas-CLOVER plasmids containing G4S linker and G4S (×4) linker were linearized for *in vitro* Cas-CLOVER mRNAs synthesis as described above.

Comparing Cas-CLOVER and Cas9 editing at multiple loci

Human pan-T cells were thawed into TCCM medium (10% FBS, 25 mM HEPES, 1× Glutamax, 1× NEAA, 1× sodium pyruvate, 55 μM 2-mercaptoethanol, RPMI 1640) and rested overnight at 37°C. On the second day, cells were spun down at 300 × *g* for 10 min and were then washed with pre-warmed Opti-MEM reduced-serum medium (Thermo Fisher) and were then resuspended in Opti-MEM for electroporation. Cells were electroporated with the BTX electroporator (BTX) to deliver Cas-CLOVER or Cas9 mRNA into cells, using the following conditions: 700 μs, 500 V, 20 μg each well, 5×10^6 cells per well. Cells were then rested in TCCM at 32°C overnight. On the third day, cells were spun down at 300× *g* for 10 min and then washed with pre-warmed Opti-MEM. Cells were electroporated as above with 10 μg of gRNA in each well and rested in TCCM at 32°C overnight. On the fourth day, cells were activated with pre-washed Dynabeads Human T-Expander CD3/CD28 (Thermo Fisher, catalog #11141D) (30 μL per 1×10^6 cells) and interleukin-2 (IL-2) was added to a final concentration of 50 U/mL to the culture and cells incubated at 37°C. Six days after electroporation, cells were stained with antibodies against the indicated markers (PD1, TGFBR2, LAG3, TIM3, CTLA4) and assayed by flow cytometry on a BD FACSCelesta (BD Biosciences, San Jose, CA).

Off-target nuclease activity at computationally predicted sites

Off-target sites were computationally predicted using a multiple inverted index strategy (KBioBox, Worcester, MA). Genomic patterns were inferred considering Cas-CLOVER binding specifics. This pattern was used to query the human genome (GRCh38p7) to identify all possible Cas-CLOVER binding sites. From the list of binding sites and locations, inverted indices were created and stored in databases on KBioBox's Web-accessible bio-informatic analysis platform. With all possible Cas-CLOVER sites stored as multiple inverted indices, and given a target Cas-CLOVER sequence, the KBioBox system identified candidate off-target locations with a range of off-target matches. PCR primers were designed to assay each site by amplicon-seq, with a total of 79 amplicons, including three on-target sites, along with 25 *B2M*, 26 *TRAC*, and 25 *PDCD1* off-target sites. PCR primer sequences are listed in Table S1. Barcoded PCR products from various samples were pooled, purified, and sequenced by NGS at the Washington University Genome Technology Access Center (Saint Louis, MO). Quality control, alignment to the reference amplicons, indel profiles, and counts per sample were performed by Desktop Genetics (London, UK). This entailed quality-based base trimming and filtering of raw FASTQ sequencing files, followed by pairwise alignment using a Needleman-Wunsch algorithm[55] with a minimum alignment score >66. Amplicon data were examined for indels if at least 5,000 mapped reads were generated at the predicted cut site.

Production of allogeneic CAR-T cells

P-BCMA-ALLO1 lots were produced using fresh apheresis product after positive immunomagnetic enrichment of CD4 and CD8 T cells. For this, an automated enrichment protocol using CliniMACS CD4 MicroBeads and CliniMACS CD8 MicroBeads was run on a CliniMACS Prodigy Instrument (Miltenyi Biotec) using a custom positive enrichment protocol. Enriched T cells were cryopreserved in a mixture of Hank's balanced salt solution (HBSS), human serum albumin (HSA), and dimethyl sulfoxide (DMSO) before storage in liquid nitrogen vapor phase.

Prior to electroporation, enriched T cells were thawed in T cell expansion medium and recovered overnight at 37°C. T cells were then resuspended in supplemented P3 Primary Cell Nucleofector solution (Lonza Group). For each electroporation reaction, mRNAs encoding super piggyBac (SPB), Cas-CLOVER (CC), synthetic, chemically modified gRNAs targeting the *TRBC1/2* and *B2M* genes, as well as a DNA piggyBac transposon plasmid encoding the CAR, a DHFR selection cassette, and the inducible Caspase-9 (iCasp) safety switch, which dimerizes in the presence of rimiducid (AP1903), were preloaded into 100 μL of Nucleocuvette vessel (Lonza Group). Cell suspensions were added, and vessels were electroporated using a 4D-Nucleofector system (Lonza Group). Post electroporation, cells were recovered in supplemented medium. The process was repeated to provide sufficient material for a total culture of multiple G-Rex 100M vessels (Wilson Wolf Corporation). Cells were incubated overnight. After electroporation and extended resting time for recovery, cells were activated through the TCR. Following activation, fresh culture medium supplemented with MTX was added to the cultures. No cytokines were added for activation, at media changes, or upon MTX addition.

The culture was maintained and supplemented with fresh media throughout the culture period to ensure sufficient nutrients were provided for the cell expansion. Cell harvest was performed once the cells exited exponential growth phase and entered the stationary phase.

The cell product was subjected to immunomagnetic depletion of residual TCR-positive CAR-T cells. After this purification step, the final cell product was cryopreserved in a mixture of HBSS, HSA, and DMSO before storage in liquid nitrogen vapor phase. Controls used for experiments were either unmodified pan-T cells or unedited CAR-T cells, in which case Cas-CLOVER and gRNAs were omitted, but MTX selection was still performed to select for transposed CAR-T cells.

Cytotoxicity assay

CAR-T cells were thawed and resuspended in RPMI 1640 medium (catalog #11874119, Gibco), supplemented with 10% FBS (catalog #F4135, Sigma-Aldrich) and 2 mM Glutamax (catalog #35050061, Gibco) (RPMI-10). Cells were counted after thaw using the Luna-FL Dual Fluorescence Cell Counter (Logos Biosystems) (acridine orange/propidium iodide exclusion).

K562 cells expressing BCMA/CBG99/GFP (K562-BCMA) or CGB99/GFP (K562 control) were used as BCMA-positive or -negative target

cells, respectively, in both the cytotoxicity and IFNγ ELISA assays. Both target cells were thawed in RPMI-10 and incubated at 37°C and 5% CO_2. After 72 h, logarithmic phase cultures were counted, pelleted, and resuspended in RPMI 1640 medium containing no phenol red (catalog #11835030, Gibco), supplemented with 10% FBS (catalog #F4135, Sigma-Aldrich) and 2mM Glutamax (catalog #35050061, Gibco) (phenol-free RPMI-10) at a concentration of 5×10^4 cells/mL.

CAR-T cells were pelleted and resuspended in phenol-free RPMI-10 at a concentration of 2×10^6 cells/mL. Two-hundred microliters of cells were plated in triplicate in the top row of a 96-well U-bottom polypropylene plate (Corning). The remainder of the plate was filled with 100 mL of assay medium and the top row was serially diluted 2:1 to create an effector cell titration. Three columns of wells were maintained with cell culture medium only (no CAR-T). One-hundred milliliters of target or control K562 cells were plated on top of all wells, mixed, and incubated at 37°C and 5% CO_2 for 48 ± 2 h. At the end of incubation, plates were centrifuged at $300 \times g$ for 5 min at room temperature and the supernatants were transferred to a separate 96-well plate and frozen at −20°C. To develop the cytotoxicity assay, reagents from the Luciferase Assay System (catalog #E1500, Promega) were brought to room temperature. Cells were lysed with 50 mL of 1X Cell Culture Lysis Reagent, mixed, and transferred to a white flat-bottom 96-well plate. Forty microliters of luciferase assay reagent was added to each well and allowed to incubate at room temperature for 5 min before reading on the Biotek Synergy in luminescence mode. The amount of light produced from each well is directly proportional to the number of surviving cells. Percentage of targets surviving at 48 h was calculated by dividing the luciferase signal remaining in each well by the average luciferase signal from target-alone wells and multiplying by 100 (assay well signal/mean tumor-only wells signal). Percentage of targets killed was calculated by subtracting the percentage surviving cells from 100. All data were exported to Microsoft Excel and plotted in GraphPad Prism.

In vivo cytotoxicity assay

In vivo efficacy of CAR-T cells was evaluated using the RPMI 8226 human multiple myeloma model in NSG (NOD.Cg-Prkdc^{scid} Il2rg^{tm1Wjl}/SzJ) mice. To establish tumors, 1×10^7 RPMI 8226 tumor cells (ATCC) were subcutaneously injected per animal into 7- to 8-week-old female NSG mice (The Jackson Laboratory, Sacramento, CA) in the right axilla on day 0. On day 7, all animals were distributed into study groups based on caliper measurement estimation of tumor burden. The mean tumor burden for all groups ranged from 75–125 mm^3.

A single dose of CAR-T was injected intravenously on day 7, with each lot assessed at 1×10^7 CAR-T cells. Mice in the PBS (no CAR-T control) groups were injected intravenously with 200 μL of PBS. Animal health checks were conducted daily. Water and food were provided *ad libitum*. Animal weight was measured three times per week. Tumors were measured via caliper three times per week. Animals were euthanized when one of the following criteria were met: (1) mean group tumor burdens reached a value between 1,500 and 2,000 mm^3, (2) body weight loss was greater than 20%, or (3) at study termination. The study was terminated on day 56. Whole blood was collected from anaesthetized mice via retro-orbital sinus into K_2EDTA MiniCollect tubes (VWR) weekly starting on day 7. At the time of euthanasia, terminal samples were collected. Terminal sampling included 500 μL of whole blood collected via cardiac puncture, bone marrow, and spleen. All samples were shipped overnight on cold packs for immediate processing at Poseida Therapeutics.

IFNγ ELISA

To measure IFNγ production from P-BCMA-ALLO1, the ELISA MAX Deluxe Set Human IFNγ kit (catalog #430104, BioLegend) was run according to manufacturer's instructions. Supernatants from the cytotoxicity assay were thawed on ice and mixed before diluting 100-fold and applying to coated ELISA plates. Developed ELISA plates were read on the Biotek Synergy in absorbance mode at 450 and 570 nm. The absorbance at 450 nm in each well is directly proportional to the amount of IFNγ in the supernatant.

Flow cytometric analysis of memory marker surface expression

For the assessment of surface and memory phenotype markers expressed on CAR-T cells, cryopreserved cells were thawed and assayed immediately or rested in T cell expansion medium for 48 h before assaying. For all lots, 5×10^5 cells were washed and resuspended in FACS buffer (PBS supplemented with 2% FBS [catalog #F4135, Sigma-Aldrich]). Cells were stained with LIVE/DEAD Fixable Aqua Dead Cell Stain Kit (catalog #L34957, Thermo Fisher Scientific) as well as antibodies for CD4, CD8, CD3, B2M, CD45RA, CD45RO, and CD62L for 30 min on ice, in the dark. Cells were washed in FACS buffer and samples were analyzed on a FACSCelesta flow cytometer (Becton, Dickinson and Company). Flow cytometric analyses was performed using BD FACS Diva (BD Biosciences) and FlowJo v10.5.3 (BD Biosciences) software. All data were graphed and analyzed using GraphPad Prism software. WT CD4+/CD8+ T cells and fluorescence minus one (FMO) controls were used to gate surface and memory cell markers. In this assay, CD3 is used as a proxy for *TCRβ1* knockout.

Assessment of KO via flow cytometry

Cell surface expression levels of the TCR complex and MHC class I were assessed by flow cytometric analysis of CD3 and B2M, respectively. T cells were stained with mouse monoclonal antibodies (BioLegend) and acquired for analysis on a BD FACSCelesta (BD Biosciences).

Identification of candidate Cas-CLOVER off-targets

The assay protocol was adopted from iGUIDE-seq.[28] Ligation-compatible, exonuclease-resistant dsODN was generated by annealing sense and anti-sense oligos using the protocol described in Nobles, 2019.[28] Briefly, the oligos were dissolved in nuclease-free water to 1 mM concentration. Equimolar concentrations of the oligos were mixed and heated to 95°C for 1 min and gradually cooled down to 4°C at the rate of −0.5°C per 90 s. The DNA duplex was stored in aliquots at −20°C until nucleofection. For oligo capture, T cells were

electroporated using a Lonza 4D-Nucleofector to deliver piggyBac transposase mRNA, Cas-CLOVER mRNA, synthetic gRNA pairs directed against *B2M* and *TRBC1/2* genes, a piggyBac transposon plasmid encoding the CAR, a chemo-selection gene, and a safety switch as well as the dsODN. Cells were then expanded and selected with MTX as described above. No-nuclease control cells were generated as described for oligo capture with the exception that Cas-CLOVER mRNA was omitted from the electroporation reaction.

Cells were collected by centrifugation and genomic DNA was extracted. Genomic regions containing the intended target sites on *B2M*, *TRBC1*, and *TRBC2* were amplified and barcoded by multiplex PCR using two primer pairs, as well as primers compatible with Illumina flowcell. PCR products from various samples were pooled, purified, and sequenced by NGS using NextSeq (Illumina). On-target modifications were quantified in terms of bases deleted using a variant detection and calling program at an allele frequency of 0.1% and an allele depth of 10 unique molecular index (UMI) reads. Samples with robust on-target activity were subjected to iGUIDE-seq library preparation using a protocol adopted from Nobles et al. (2019).[28]

Raw reads were demultiplexed using bcl2fastq program. Low-quality reads with an average quality score <25 were removed. Reads were collapsed based on matching UMIs. Reads with dsODN sequence were aligned to the hg38 human genome using BWA v0.7.5a-r405. The dsODN-integration site junctions were calculated for each read. Read peaks ($\geq$10 UMI reads) were identified. Candidate Cas-CLOVER cut sites were identified by searching for doublet read peaks separated by $\leq$ 10 nucleotides. Background sites identified in the matching no-nuclease controls were subtracted from the Cas-CLOVER-treated cell samples.

To create a donor-wide list of candidate off-targets, consolidation of iGUIDE-seq sites was performed using a custom Python script and BEDtools suite. In this process, redundant and overlapping sites were merged to create a unique set of sites. Briefly, based on genomic coordinates, sites lying within a 150-bp vicinity were merged within each replicate. Technically reproducible sites (sites occurring in at least two technical replicates among all donors) were pooled and merged again as described above. This pipeline included candidate sites that failed to reproduce across technical replicates but that were reproduced across at least two donors. GUIDE-seq capture sites are listed in Table S2.

Amplicon sequencing and quantification of Cas-CLOVER activity

Cas-CLOVER activity at on-target and at candidate off-target sites was assessed by targeted amplicon-seq. The primer and amplicon design, NGS, and indel quantification was performed by Genenius Genetics (San Diego, CA). The cell samples were thawed and collected by centrifugation. Genomic DNA was extracted and genomic regions containing the target sites were amplified by multiplex PCR using two primer sets per site using 330 ng of input genomic DNA per reaction. Sites BA1-GS18 and BA1-GS58 map to a genomic EEF1A1 site that is 99% identical to the CAR transposon promoter. To enrich genomic sites, these sites were amplified in a two-step PCR approach. In the first PCR, a pair of primers targeting the genomic locus were designed and were used to pre-enrich the region in a 1.7-kb fragment. A small fraction of the pre-enrichment reaction was used for the following PCRs for amplicon-seq. The rest of the sites used standard amplicon-seq primer design. Barcoded PCR products from various samples were pooled, purified, and sequenced by NGS using a NextSeq (Illumina, San Diego, CA) sequencer.

The initial sequence data analysis including indel quantification was performed by Genenius Genetics. Briefly, sequence reads were demultiplexed, low-quality reads were removed by quality-score-based filtering, and PCR duplicates were collapsed by UMI-based deduplication. The quality control steps were verified by checking the read quality using FastQC. High-quality reads were then aligned to the human genome (hg38) using BWA v0.7.5a-r405 aligner. Alignments were parsed to calculate insertion and deletion variants. To detect rare indels, variants in each amplicon were called based on an allele frequency threshold of 0.01% and an allele depth of 1. Sequence alignment files (BAM) and the indel counts were then provided by Genenius Genetics for the downstream analysis. Normalized indel counts obtained by background correction were also provided by the contract research organization (CRO). At low allele frequency thresholds, noise in sequencing data tends to increase the chances of detecting false-positives. To avoid such false-positives, a statistical analysis described in Pattanayak (2011)[56] and a multiple testing correction was performed. Bonferroni-corrected p values along with total and indel-containing reads are provided in the supplementary tables. Although Bonferroni correction reduces a lot of false-positives, the correction might eliminate true-positives. To avoid losing such sites, we performed an unbiased, semi-automated visual examination of sequence read alignments for identifying true DSB events across all the sites. Sites with skewed read coverage in treated over the control samples ($\geq$1.2-fold) and reads with 1-bp deletion, which can result from PCR, sequencing, and primer synthesis artifacts, were excluded from this analysis. Sites with $\geq$3 unique overlapping indel events in at least five unique reads in treated samples with no indels in the donor-matched controls were considered as sites of true cutting. The center of the stacked indels, which is the expected Cas-CLOVER cut site, was used for gene and gene feature annotations and assessment of functional consequences of off-target cutting.

For indel profile analysis, a Python-based custom script was used to process sequence alignment (BAM) files generated upon the mapping of unique reads by the CRO. Briefly, indel variants were calculated per base using the Pysam package. Variant counts were normalized to read depth and displayed using Matplotlib package in Python. Deletion sizes per read were simultaneously calculated. Results from amplicon-seq are listed in Table S3.

Assessment of translocations by AMP-seq

The method used to detect translocation events was an adaptation of standard anchored multiplex PCR (AMP)-based NGS assay.[29] To

improve the sensitivity and reduce DNA loss during the processes, the amount of input gDNA was scaled up from 50 ng to 2 μg. This change increased the input from ~15,000 to ~600,000 haploid human genomes. Samples were processed in batches of 500 ng and the libraries were pooled before sequencing.

The sequence data analysis and quantification of translocation junctions were performed in collaboration with Genenius Genetics. Briefly, sequence reads were demultiplexed, low-quality reads were removed by quality-score-based filtering, and PCR duplicates were collapsed by UMI-based deduplication. The quality control steps were verified by checking the read quality using FastQC. High-quality reads were aligned to the human genome (hg38) using BWA v0.7.5a-r405 aligner and the translocation junctions between on-to-on and on-to-verified-off targets were identified and quantified. Circos plots were plotted using translocation junction counts normalized to the total reads using RCircos package (v1.2.1) in R. Results from the translocation analysis are listed in Table S4.

Knockin evaluation in iPSCs

Human induced pluripotent stem cells (iPSCs) (Thermo Fisher Scientific, catalog #A18945) were maintained on tissue culture plates coated with human embryonic stem cell (hESC)-qualified Matrigel (Corning, catalog # 354277) with mTeSR Plus medium (StemCell Technologies, catalog #100-0276) and passaged twice a week by dissociation with EDTA. For introduction of gene editing components and donor cassettes, cells were pre-treated with the ROCK (Rho kinase) inhibitor Y-27632 (StemCell Technologies, catalog #72302) for at least 1 h before dissociation into single cells by TrypLE Express (Thermo Fisher Scientific, catalog #12604054) and subject to nucleofection via the P3 Primary Cell 4D-Nucleofector X Kit (Lonza, catalog #V4XP-3024) using program CA-137. From 500,000 to 800,000 cells were nucleofected for each 100-μL reaction, with Cas-CLOVER or HiFiCas9 mRNA (5 μg), genome targeting single guide RNAs (sgRNAs) (2 μg), and/or HDR donor plasmids (1–4 μg). For experiments involving Cas9 protein (3 μg per reaction; IDT, catalog #1081058), ribonucleoproteins (RNPs) were pre-assembled at room temperature in P3 buffer for 15 min before nucleofection. HDR donor plasmids were designed to deliver turboGFP-T2A (targeting *GAPDH*), T2A-turboGFP-BGHpA (targeting *B2M*), and UBC-turboGFP-BGHpA (targeting *HBB*), and are flanked by locus-specific homology arms.

For indel analysis, cells were collected 3 days post nucleofection. Genomic DNA was extracted (Zymo, catalog #D3024) and locus-specific sequences encompassing the genomic cut sites were amplified by PCR. The amplicons were subjected to Sanger sequencing (Eton Bioscience) followed by analysis using Inference of CRISPR Edits (ICE; Synthego). For HDR analysis, cells were collected 3 to 15 days post nucleofection. For the *GAPDH* and *HBB* loci, GFP expression was assessed by flow cytometry (BD FACSCelesta). For the *B2M* locus, genomic DNA was extracted and HDR measured by a probe-based droplet digital PCR (ddPCR) system (Bio-Rad). Predesigned HDR reference primer/probe sets (HEX) were purchased from Bio-Rad (#12003806, dHsaRFS96350745, human EIF2C1 603). *B2M* HDR detection set (FAM) was designed in house and synthesized by IDT. The ddPCR assays were conducted according to the manufacturer's guidelines, except a 2-min extension step at 72°C was added, following the 1-min annealing step at 60°C.

Karyotype via G-banding

This procedure was carried out at Karyologic (Durham, NC). Cryopreserved T cell samples were thawed and stimulated in medium supplemented with PMA (phorbol myristate acetate) and ionomycin for 4 to 5 days. Cultures were incubated with Colcemid at a final concentration of 0.5 μg/mL, at 37°C, 5% CO_2, for 60 to 90 min. Cells were centrifuged at 300 × *g* for 7 min and resuspended in 0.075 M KCl hypotonic solution, incubated at ambient temperature for 7 min, and centrifuged at 300 × *g* for 7 min. Cells were resuspended in 3:1 methanol/acetic acid fixative, incubated at ambient temperature for 15 min, and centrifuged at 300 × *g* for 7 min. The fixative step was repeated, and fixed cell samples stored at 3°C to 6°C for at least 24 h before making slides.

To prepare microscope slides of metaphase chromosome spreads, the methanol/acetic acid storage fixative was replaced with fresh fixative and cells were centrifuged at 300 × *g* for 7 min. Cells were resuspended and dropped onto microscope slides. Slides were incubated at 65°C for 20 h, cooled, then washed for 1 min in trypsin-EDTA, followed by quick rinses in 2% FBS in 1× PBS, 1× PBS, and distilled water. Slides were soaked with freshly made Giemsa stain, diluted 1:5 in Gurr's buffer, pH 6.8, for 15 s, and rinsed in distilled water and dried. Two-hundred metaphase spreads were analyzed for each sample at 1,000× using a Leica brightfield microscope DM2500 equipped with a CCD (charge-coupled device) camera and Leica Microsystems CytoVision Karyotyping Software.

Directional genomic hybridization and imaging

This procedure was carried out at KromaTiD (Longmont, CO). Cryopreserved T cell samples were thawed and stimulated in medium supplemented with PMA and ionomycin for 4 days. For directional genomic hybridization (dGH), 5.0 mM 5-bromo-deoxyuridine (BrdU) and 1.0 mM 5-bromo-deoxycytidine (BrdC) were added to the culture media on day 4 for the duration of one cellular division cycle. At 4 h prior to harvest, Colcemid was added to a final concentration of 0.1 μg/mL to each sample. The samples were harvested and fixed in methanol/acetic acid and metaphase spreads were prepared for each sample using standard cytogenetic techniques.[33]

Metaphase spread preparations singly substituted with bromodeoxynucleotides (BrdU and BrdC) were submersed in Hoechst 33258 for 15 min, selectively photolyzed using a SpectroLinker XL 1500 UV Crosslinker equipped with 365-nm UV bulbs for 35 min, followed by exonucleolytic degradation of the nicked DNA with exonuclease III for 35 min, to remove the newly replicated strand in each metaphase chromosome. An assay composed of dGH chromatid paints for human chromosomes 1, 2, and 3 labeled in ATTO-550, custom targeted probes bracketing the edit site at *TRBC* in ATTO-425, and

the edit site at *B2M* in ATTO-647 was assembled with hybridization buffer and applied to the slides and denatured at 68°C for 3 min. Probe sets targeting *TRBC1/2* cover a 290-kb centromeric region (chr7:141,746,769-142,036,955, at a distance of 755 kb from the edit site) and a 642-kb telomeric region (chr7:143,095,575-143,737,207, at a distance of 304 kb from the edit site). Probe sets targeting *B2M* cover a 380-kb centromeric region (chr15:43,577,282-43,956,866, at a distance of 755 kb from the edit site) and a 318-kb telomeric region (chr15:45,083,350-45,401,601, at a distance of 690 kb from the edit site). Slides were hybridized overnight at 37°C followed by five washes in 2× saline-sodium citrate at 43°C prior to imaging. Metaphase spreads were imaged on an Applied Spectral Imaging Harmony system using a Zeiss Axio Imager.Z2m microscope equipped with a Basler acA2440-35um camera and a Lumencor SOLA SE-FISH LED light source, using a 100× objective. The resulting images were scored for translocation, inversions/sister-chromatid exchanges (SCEs), deletions, and other complex structural rearrangements using defined scoring rules.

Scoring rules for dGH microscopy

Metaphase spreads were visually inspected to verify that each chromosome with signal can be distinctly discriminated and visualized separately from others (e.g., overlapping in a "pile"). Spreads with little to no spacing between chromosomes were disqualified, as were partial spreads in which chromosome(s) were missing, or for spreads in which chromosome(s) were too far away to be imaged in a single field. Spreads with fewer than 40 or more than 50 chromosomes were disqualified from scoring. Spreads were also disqualified if one chromatid had brighter DAPI staining relative to the sister chromatid. For all chromosome scoring, the reviewer was blinded to the nature and identity of each sample.

For probe signal from chromosome 7 (*TRBC*, aqua probe) and 15 (*B2M*, yellow probe) edit site spreads are scored as having an inversion/SCE if the respective probes are found on the opposite sister chromatids. Translocations are scored when probe signal is found on another chromosome, with translocations between edit sites at *TRBC* and *B2M* having co-localized aqua and yellow probe signals. Probe signals found on another chromosome, which do not appear to reflect translocations, are scored as insertions.

For whole-chromosome paints of chromosomes 1, 2, and 3, their similarity in size prohibited their discrimination from one another. These whole-chromosome paints (also called dosimetry paints) are expected only on one chromatid. For these dosimetry-labeled chromosomes, translocations were defined when a part of the fluorescent signal from a labeled sister-chromatid complex appears attached to another unlabeled chromosome. Inversions or SCEs were evident when one or more signal was present on the unlabeled side of a sister chromatid. These two events, inversions versus SCEs, cannot be distinguished from each other. Insertions of dosimetry painted chromosomes were evident when such signal appears within an unlabeled chromosome. Any rearrangements or abnormalities that did not meet the defined criteria above were scored as complex.

Mixed lymphocyte reaction

Responder cells were labeled with cell trace violet (CTV) dye. Irradiated stimulator cells were labeled with carboxyfluorescein diacetate succinimidyl ester (CFSE) dye. Successful dye labeling of both stimulator and responder cells was assessed via flow cytometric analysis following the labeling reaction. For the mixed lymphocyte reaction (MLR), irradiated stimulator cells from three donors were paired in cocultures with allogeneic CAR-T cells or TCR+ unmodified T cells from the same donor. For each stimulator-responder pair, cells were cocultured at a stimulator:responder ratio of 1:2 for 7 days. After 7 days of co-culture, CTV dye dilution was assessed via flow cytometry. Unstimulated, CTV-labeled T cells that were not exposed to stimulator cells were used as a reference.

MM1S xenograft model

CAR-T *in vivo* efficacy was evaluated using the luciferase-expressing MM.1S human systemic multiple myeloma model in NSG mice. To establish tumors, 3×10^5 MM.1S-Luc-Neo tumor cells were intravenously injected into 7- to 8-week-old female NSG mice on day 0. On day 6, animals were sorted into treatment groups based on tumor burden as assessed by bioluminescence imaging (BLI). On day 7, a single dose of 12×10^6 CAR-T was injected intravenously (n = 7 per group). Survival bleeds were performed on days 5, 12, 19, 28, 47, and 63 after CAR-T infusion and circulating human T cells were quantified. Animal studies were reviewed and received approval by the institutional animal care and use committee at the contract research organization assisting with these mouse experiments.

SUPPLEMENTAL INFORMATION

Supplemental information can be found online at https://doi.org/10.1016/j.omtn.2022.06.003.

ACKNOWLEDGMENTS

Poseida Therapeutics is the sole agency/body responsible for funding and performing this research. The authors have competing interests because of current employment, previous employment, stock ownership, and/or the right to exercise stock options with Poseida Therapeutics, which stands to gain financially through the publication of this manuscript.

AUTHOR CONTRIBUTIONS

E.M.O., D.J.S., B.B.M., J.C., D.P., M.R., H.X., X.L., and S.C. designed the work and participated in the analysis and interpretation of data. B.B.M., D.P., and M.R. drafted the manuscript. D.P., M.R., S.C., X.W., Y.T., L.W., R.M., H.X., M.T., and K.M. participated in the execution of experiments and the acquisition of data. E.M.O., D.J.S., B.B.M., and J.C. provided editorial input for final composition of the manuscript draft.

DECLARATION OF INTERESTS

The authors have competing interests because of current employment, previous employment, stock ownership, and/or the right to exercise stock options with Poseida Therapeutics.

REFERENCES

1. Kalos, M., Levine, B.L., Porter, D.L., Katz, S., Grupp, S.A., Bagg, A., and June, C.H. (2011). T cells with chimeric antigen receptors have potent antitumor effects and can establish memory in patients with advanced leukemia. Sci. Transl. Med. *3*, 95ra73.
2. Ali, S.A., Shi, V., Maric, I., Wang, M., Stroncek, D.F., Rose, J.J., Brudno, J.N., Stetler-Stevenson, M., Feldman, S.A., Hansen, B.G., et al. (2016). T cells expressing an anti-B-cell maturation antigen chimeric antigen receptor cause remissions of multiple myeloma. Blood *128*, 1688–1700.
3. Verma, R., Foster, R.E., Horgan, K., Mounsey, K., Nixon, H., Smalle, N., Hughes, T.A., and Carter, C.R. (2016). Lymphocyte depletion and repopulation after chemotherapy for primary breast cancer. Breast Cancer Res. *18*, 10.
4. Ran, F.A., Hsu, P.D., Wright, J., Agarwala, V., Scott, D.A., and Zhang, F. (2013). Genome engineering using the CRISPR-Cas9 system. Nat. Protoc. *8*, 2281–2308.
5. Pattanayak, V., Lin, S., Guilinger, J.P., Ma, E., Doudna, J.A., and Liu, D.R. (2013). High-throughput profiling of off-target DNA cleavage reveals RNA-programmed Cas9 nuclease specificity. Nat. Biotechnol. *31*, 839–843.
6. Hsu, P.D., Scott, D.A., Weinstein, J.A., Ran, F.A., Konermann, S., Agarwala, V., Li, Y., Fine, E.J., Wu, X., Shalem, O., et al. (2013). DNA targeting specificity of RNA-guided Cas9 nucleases. Nat. Biotechnol. *31*, 827–832.
7. Ran, F.A., Hsu, P.D., Lin, C.Y., Gootenberg, J.S., Konermann, S., Trevino, A.E., Scott, D.A., Inoue, A., Matoba, S., Zhang, Y., and Zhang, F. (2013). Double nicking by RNA-guided CRISPR Cas9 for enhanced genome editing specificity. Cell *155*, 479–480. https://doi.org/10.1016/j.cell.2013.09.040.
8. Ren, J., Liu, X., Fang, C., Jiang, S., June, C.H., and Zhao, Y. (2017). Multiplex genome editing to generate universal CAR T cells resistant to PD1 inhibition. Clin. Cancer Res. *23*, 2255–2266. https://doi.org/10.1158/1078-0432.ccr-16-1300.
9. Bothmer, A., Gareau, K.W., Abdulkerim, H.S., Buquicchio, F., Cohen, L., Viswanathan, R., Zuris, J.A., Marco, E., Fernandez, C.A., Myer, V.E., and Cotta-Ramusino, C. (2020). Detection and modulation of DNA translocations during multi-gene genome editing in T cells. CRISPR J *3*, 177–187. https://doi.org/10.1089/crispr.2019.0074.
10. Webber, B.R., Lonetree, C.L., Kluesner, M.G., Johnson, M.J., Pomeroy, E.J., Diers, M.D., Lahr, W.S., Draper, G.M., Slipek, N.J., Smeester, B.A., et al. (2019). Highly efficient multiplex human T cell engineering without double-strand breaks using Cas9 base editors. Nat. Commun. *10*, 5222. https://doi.org/10.1038/s41467-019-13007-6.
11. Giannoukos, G., Ciulla, D.M., Marco, E., Abdulkerim, H.S., Barrera, L.A., Bothmer, A., Dhanapal, V., Gloskowski, S.W., Jayaram, H., Maeder, M.L., et al. (2018). UDiTaS, a genome editing detection method for indels and genome rearrangements. BMC Genom. *19*, 212. https://doi.org/10.1186/s12864-018-4561-9.
12. Gattinoni, L., Lugli, E., Ji, Y., Pos, Z., Paulos, C.M., Quigley, M.F., Almeida, J.R., Gostick, E., Yu, Z., Carpenito, C., et al. (2011). A human memory T cell subset with stem cell-like properties. Nat. Med. *17*, 1290–1297. https://doi.org/10.1038/nm.2446.
13. Fuertes Marraco, S.A., Soneson, C., Cagnon, L., Gannon, P.O., Allard, M., Maillard, S.A., Montandon, N., Rufer, N., Waldvogel, S., Delorenzi, M., and Speiser, D.E. (2015). Long-lasting stem cell–like memory CD8 $^{+}$ T cells with a naïve-like profile upon yellow fever vaccination. Sci. Transl. Med. *7*, 282ra48. https://doi.org/10.1126/scitranslmed.aaa3700.
14. Biasco, L., Scala, S., Basso Ricci, L., Dionisio, F., Baricordi, C., Calabria, A., Giannelli, S., Cieri, N., Barzaghi, F., Pajno, R., et al. (2015). In vivo tracking of T cells in humans unveils decade-long survival and activity of genetically modified T memory stem cells. Sci. Transl. Med. *7*, 273ra13. https://doi.org/10.1126/scitranslmed.3010314.
15. Gattinoni, L., Klebanoff, C.A., Palmer, D.C., Wrzesinski, C., Kerstann, K., Yu, Z., Finkelstein, S.E., Theoret, M.R., Rosenberg, S.A., and Restifo, N.P. (2005). Acquisition of full effector function in vitro paradoxically impairs the in vivo antitumor efficacy of adoptively transferred CD8+ T cells. J. Clin. Invest. *115*, 1616–1626. https://doi.org/10.1172/jci24480.
16. Klebanoff, C.A., Gattinoni, L., Torabi-Parizi, P., Kerstann, K., Cardones, A.R., Finkelstein, S.E., Palmer, D.C., Antony, P.A., Hwang, S.T., Rosenberg, S.A., et al. (2005). Central memory self/tumor-reactive CD8+ T cells confer superior antitumor immunity compared with effector memory T cells. Proc. Natl. Acad. Sci. USA *102*, 9571–9576. https://doi.org/10.1073/pnas.0503726102.
17. Hinrichs, C.S., Borman, Z.A., Cassard, L., Gattinoni, L., Spolski, R., Yu, Z., Sanchez-Perez, L., Muranski, P., Kern, S.J., Logun, C., et al. (2009). Adoptively transferred effector cells derived from naïve rather than central memory CD8 $^{+}$ T cells mediate superior antitumor immunity. Proc. Natl. Acad. Sci. USA *106*, 17469–17474. https://doi.org/10.1073/pnas.0907448106.
18. Sabatino, M., Hu, J., Sommariva, M., Gautam, S., Fellowes, V., Hocker, J.D., Dougherty, S., Qin, H., Klebanoff, C.A., Fry, T.J., et al. (2016). Generation of clinical-grade CD19-specific CAR-modified CD8+ memory stem cells for the treatment of human B-cell malignancies. Blood *128*, 519–528. https://doi.org/10.1182/blood-2015-11-683847.
19. Guan, L., Li, X., Wei, J., Liang, Z., Yang, J., Weng, X., and Wu, X. (2018). Antigen-specific CD8+ memory stem T cells generated from human peripheral blood effectively eradicate allogeneic targets in mice. Stem Cell Res. Ther. *9*, 337. https://doi.org/10.1186/s13287-018-1080-1.
20. Pilipow, K., Scamardella, E., Puccio, S., Gautam, S., De Paoli, F., Mazza, E.M., De Simone, G., Polletti, S., Buccilli, M., Zanon, V., et al. (2018). Antioxidant metabolism regulates CD8+ T memory stem cell formation and antitumor immunity. JCI Insight *3*, 122299. https://doi.org/10.1172/jci.insight.122299.
21. Ando, M., Ikeda, M., Yoshimura, A., and Kondo, T. (2020). *In vitro* generation of stem cell memory-like T cells from activated T cells. Methods Mol. Biol. *2111*, 127–139. https://doi.org/10.1007/978-1-0716-0266-9_11.
22. Kondo, T., Ando, M., Nagai, N., Tomisato, W., Srirat, T., Liu, B., Mise-Omata, S., Ikeda, M., Chikuma, S., Nishimasu, H., et al. (2020). The NOTCH-FOXM1 Axis plays a key role in mitochondrial biogenesis in the induction of human stem cell memory-like CAR-T cells. Cancer Res. *80*, 471–483. https://doi.org/10.1158/0008-5472.can-19-1196.
23. Verma, V., Jafarzadeh, N., Boi, S., Kundu, S., Jiang, Z., Fan, Y., Lopez, J., Nandre, R., Zeng, P., Alolaqi, F., et al. (2021). MEK inhibition reprograms CD8(+) T lymphocytes into memory stem cells with potent antitumor effects. Nat. Immunol. *22*, 53–66. https://doi.org/10.1038/s41590-020-00818-9.
24. Kotowski, M., and Sharma, S. (2020). CRISPR-based editing techniques for genetic manipulation of primary T cells. Methods Protoc. *3*, 79. https://doi.org/10.3390/mps3040079.
25. Yi, G., Choi, J.G., Bharaj, P., Abraham, S., Dang, Y., Kafri, T., Alozie, O., Manjunath, M.N., and Shankar, P. (2014). CCR5 gene editing of resting CD4(+) T cells by transient ZFN expression from HIV envelope pseudotyped nonintegrating lentivirus confers HIV-1 resistance in humanized mice. Mol. Ther. Nucleic Acids *3*, e198. https://doi.org/10.1038/mtna.2014.52.
26. Daly, K.E., and Stephens, K.P. (2016). Method and system for rapid searching of genomic data and uses thereof. Google Patents.
27. Tsai, S.Q., Zheng, Z., Nguyen, N.T., Liebers, M., Topkar, V.V., Thapar, V., Wyvekens, N., Khayter, C., Iafrate, A.J., Le, L.P., et al. (2015). GUIDE-seq enables genome-wide profiling of off-target cleavage by CRISPR-Cas nucleases. Nat. Biotechnol. *33*, 187–197. https://doi.org/10.1038/nbt.3117.
28. Nobles, C.L., Reddy, S., Salas-McKee, J., Liu, X., June, C.H., Melenhorst, J.J., Davis, M.M., Zhao, Y., and Bushman, F.D. (2019). iGUIDE: an improved pipeline for analyzing CRISPR cleavage specificity. Genome Biol. *20*, 14. https://doi.org/10.1186/s13059-019-1625-3.
29. Zheng, Z., Liebers, M., Zhelyazkova, B., Cao, Y., Panditi, D., Lynch, K.D., Chen, J., Robinson, H.E., Shim, H.S., Chmielecki, J., et al. (2014). Anchored multiplex PCR for targeted next-generation sequencing. Nat. Med. *20*, 1479–1484. https://doi.org/10.1038/nm.3729.
30. Qasim, W., Zhan, H., Samarasinghe, S., Adams, S., Amrolia, P., Stafford, S., Butler, K., Rivat, C., Wright, G., Somana, K., et al. (2017). Molecular remission of infant B-ALL after infusion of universal TALEN gene-edited CAR T cells. Sci. Transl. Med. *9*, eaaj2013. https://doi.org/10.1126/scitranslmed.aaj2013.
31. Poirot, L., Philip, B., Schiffer-Mannioui, C., Le Clerre, D., Chion-Sotinel, I., Derniame, S., Potrel, P., Bas, C., Lemaire, L., Galetto, R., et al. (2015). Multiplex genome-edited T-cell manufacturing platform for "Off-the-Shelf" adoptive T-cell immunotherapies. Cancer Res. *75*, 3853–3864. https://doi.org/10.1158/0008-5472.can-14-3321.
32. Ray, F.A., Zimmerman, E., Robinson, B., Cornforth, M.N., Bedford, J.S., Goodwin, E.H., and Bailey, S.M. (2013). Directional genomic hybridization for chromosomal

inversion discovery and detection. Chromosome Res. *21*, 165–174. https://doi.org/10.1007/s10577-013-9345-0.

33. Howe, B., Umrigar, A., and Tsien, F. (2014). Chromosome preparation from cultured cells. J Vis Exp, e50203. https://doi.org/10.3791/50203.

34. Gautron, A.S., Juillerat, A., Guyot, V., Filhol, J.M., Dessez, E., Duclert, A., Duchateau, P., and Poirot, L. (2017). Fine and predictable tuning of TALEN gene editing targeting for improved T cell adoptive immunotherapy. Mol. Ther. Nucleic Acids *9*, 312–321. https://doi.org/10.1016/j.omtn.2017.10.005.

35. Stadtmauer, E.A., Fraietta, J.A., Davis, M.M., Cohen, A.D., Weber, K.L., Lancaster, E., Mangan, P.A., Kulikovskaya, I., Gupta, M., Chen, F., et al. (2020). CRISPR-engineered T cells in patients with refractory cancer. Science *367*, eaba7365. https://doi.org/10.1126/science.aba7365.

36. Kleinstiver, B.P., Sousa, A.A., Walton, R.T., Tak, Y.E., Hsu, J.Y., Clement, K., Welch, M.M., Horng, J.E., Malagon-Lopez, J., Scarfò, I., et al. (2019). Engineered CRISPR-Cas12a variants with increased activities and improved targeting ranges for gene, epigenetic and base editing. Nat. Biotechnol. *37*, 276–282. https://doi.org/10.1038/s41587-018-0011-0.

37. Wiebking, V., Lee, C.M., Mostrel, N., Lahiri, P., Bak, R., Bao, G., Roncarolo, M.G., Bertaina, A., and Porteus, M.H. (2021). Genome editing of donor-derived T-cells to generate allogenic chimeric antigen receptor-modified T cells: optimizing αβ T cell-depleted haploidentical hematopoietic stem cell transplantation. Haematologica *106*, 847–858. https://doi.org/10.3324/haematol.2019.233882.

38. Georgiadis, C., Rasaiyaah, J., Gkazi, S.A., Preece, R., Etuk, A., Christi, A., and Qasim, W. (2021). Base-edited CAR T cells for combinational therapy against T cell malignancies. Leukemia *35*, 3466–3481. https://doi.org/10.1038/s41375-021-01282-6.

39. Grünewald, J., Zhou, R., Iyer, S., Lareau, C.A., Garcia, S.P., Aryee, M.J., and Joung, J.K. (2019). CRISPR DNA base editors with reduced RNA off-target and self-editing activities. Nat. Biotechnol. *37*, 1041–1048. https://doi.org/10.1038/s41587-019-0236-6.

40. Doman, J.L., Raguram, A., Newby, G.A., and Liu, D.R. (2020). Evaluation and minimization of Cas9-independent off-target DNA editing by cytosine base editors. Nat. Biotechnol. *38*, 620–628. https://doi.org/10.1038/s41587-020-0414-6.

41. Yu, Y., Leete, T.C., Born, D.A., Young, L., Barrera, L.A., Lee, S.J., Rees, H.A., Ciaramella, G., and Gaudelli, N.M. (2020). Cytosine base editors with minimized unguided DNA and RNA off-target events and high on-target activity. Nat. Commun. *11*, 2052. https://doi.org/10.1038/s41467-020-15887-5.

42. Gehrke, J.M., Cervantes, O., Clement, M.K., Wu, Y., Zeng, J., Bauer, D.E., Pinello, L., and Joung, J.K. (2018). An APOBEC3A-Cas9 base editor with minimized bystander and off-target activities. Nat. Biotechnol. *36*, 977–982. https://doi.org/10.1038/nbt.4199.

43. Grünewald, J., Zhou, R., Garcia, S.P., Iyer, S., Lareau, C.A., Aryee, M.J., and Joung, J.K. (2019). Transcriptome-wide off-target RNA editing induced by CRISPR-guided DNA base editors. Nature *569*, 433–437. https://doi.org/10.1038/s41586-019-1161-z.

44. Kim, D., Kim, D.E., Lee, G., Cho, S.I., and Kim, J.S. (2019). Genome-wide target specificity of CRISPR RNA-guided adenine base editors. Nat. Biotechnol. *37*, 430–435. https://doi.org/10.1038/s41587-019-0050-1.

45. Kim, D., Lim, K., Kim, S.T., Yoon, S.H., Kim, K., Ryu, S.M., and Kim, J.S. (2017). Genome-wide target specificities of CRISPR RNA-guided programmable deaminases. Nat. Biotechnol. *35*, 475–480. https://doi.org/10.1038/nbt.3852.

46. Zuo, E., Sun, Y., Wei, W., Yuan, T., Ying, W., Sun, H., Yuan, L., Steinmetz, L.M., Li, Y., and Yang, H. (2019). Cytosine base editor generates substantial off-target single-nucleotide variants in mouse embryos. Science *364*, 289–292. https://doi.org/10.1126/science.aav9973.

47. Galvan, D.L., Nakazawa, Y., Kaja, A., Kettlun, C., Cooper, L.J.N., Rooney, C.M., and Wilson, M.H. (2009). Genome-wide mapping of PiggyBac transposon integrations in primary human T cells. J. Immunother. *32*, 837–844. https://doi.org/10.1097/cji.0b013e3181b2914c.

48. Gogol-Döring, A., Ammar, I., Gupta, S., Bunse, M., Miskey, C., Chen, W., Uckert, W., Schulz, T.F., Izsvák, Z., and Ivics, Z. (2016). Genome-wide profiling reveals remarkable parallels between insertion site selection properties of the MLV retrovirus and the piggyBac transposon in primary human CD4(+) T cells. Mol. Ther. *24*, 592–606. https://doi.org/10.1038/mt.2016.11.

49. Li, M.A., Pettitt, S.J., Eckert, S., Ning, Z., Rice, S., Cadiñanos, J., Yusa, K., Conte, N., and Bradley, A. (2013). The piggyBac transposon displays local and distant reintegration preferences and can cause mutations at noncanonical integration sites. Mol. Cell Biol. *33*, 1317–1330. https://doi.org/10.1128/mcb.00670-12.

50. Straathof, K.C., Pule, M.A., Yotnda, P., Dotti, G., Vanin, E.F., Brenner, M.K., Heslop, H.E., Spencer, D.M., and Rooney, C.M. (2005). An inducible caspase 9 safety switch for T-cell therapy. Blood *105*, 4247–4254. https://doi.org/10.1182/blood-2004-11-4564.

51. Di Stasi, A., Tey, S.K., Dotti, G., Fujita, Y., Kennedy-Nasser, A., Martinez, C., Straathof, K., Liu, E., Durett, A.G., Grilley, B., et al. (2011). Inducible apoptosis as a safety switch for adoptive cell therapy. N. Engl. J. Med. *365*, 1673–1683. https://doi.org/10.1056/nejmoa1106152.

52. Bishop, D.C., Clancy, L.E., Simms, R., Burgess, J., Mathew, G., Moezzi, L., Street, J.A., Sutrave, G., Atkins, E., McGuire, H.M., et al. (2021). Development of CAR T-cell lymphoma in 2 of 10 patients effectively treated with piggyBac-modified CD19 CAR T cells. Blood *138*, 1504–1509. https://doi.org/10.1182/blood.2021010813.

53. Micklethwaite, K.P., Gowrishankar, K., Gloss, B.S., Li, Z., Street, J.A., Moezzi, L., Mach, M.A., Sutrave, G., Clancy, L.E., Bishop, D.C., et al. (2021). Investigation of product-derived lymphoma following infusion of piggyBac-modified CD19 chimeric antigen receptor T cells. Blood *138*, 1391–1405. https://doi.org/10.1182/blood.2021010858.

54. Leibowitz, M.L., Papathanasiou, S., Doerfler, P.A., Blaine, L.J., Sun, L., Yao, Y., Zhang, C.Z., Weiss, M.J., and Pellman, D. (2021). Chromothripsis as an on-target consequence of CRISPR-Cas9 genome editing. Nat. Genet. *53*, 895–905. https://doi.org/10.1038/s41588-021-00838-7.

55. Needleman, S.B., and Wunsch, C.D. (1970). A general method applicable to the search for similarities in the amino acid sequence of two proteins. J. Mol. Biol. *48*, 443–453. https://doi.org/10.1016/0022-2836(70)90057-4.

56. Pattanayak, V., Ramirez, C.L., Joung, J.K., and Liu, D.R. (2011). Revealing off-target cleavage specificities of zinc-finger nucleases by in vitro selection. Nat. Methods *8*, 765–770. https://doi.org/10.1038/nmeth.1670.